Foldamer Metallogels: Metal Driven Supramolecular Assembly of Peptide Foldamers

Thesis submitted towards the partial fulfillment of the BS-MS dual degree programme

By,

Abhijith S. A.

20121033

Under the guidance of,

Dr. Hosahudya N. Gopi

Associate Professor, Department of Chemistry

IISER, Pune.

CERTIFICATE

This is to certify that this dissertation entitled "***Foldamer Metallogels: Metal Driven Supramolecular Assembly of Peptide Foldamers***" towards the partial fulfillment of the BS-MS dual degree programme at the Indian Institute of Science Education and Research, Pune represents original research carried out by Abhijith S. A. at IISER Pune under my supervision during the academic year 2016-2017. The work presented here or any part of it has not been included in any other thesis submitted previously for the award of any degree or diploma from any other university or institution.

20/03/2017
IISER Pune

Dr. Hosahudya N. Gopi
Associate Professor
Department of Chemistry
IISER Pune

DECLARATION

I hereby declare that the matter embodied in the report entitled "***Foldamer Metallogels: Metal Driven Supramolecular Assembly of Peptide Foldamers***" are the results of the investigations carried out by me at the Department of Chemistry, Indian Institute of Science Education and Research, Pune, under the supervision of **Dr. Hosahudya N. Gopi** and the same has not been submitted elsewhere for any other degree.

20/03/2017
IISER Pune

Abhijith S. A.
20121033
BS- MS 5th Year

ACKNOWLEDGEMENTS

I would like to place on record my deep sense of gratitude to Dr. Hosahudya N. Gopi for giving me an opportunity to learn under his guidance. I consider myself very lucky and honored to have him as my mentor for my master's thesis. His unconditional support, encouragement and informative discussions and advices had a great impact on the successful completion of this research project.

I express my sincere gratitude to my TAC member, Prof. Manickam Jayakannan for his generous guidance and fruitful suggestions.

I would also like to acknowledge all the current and previous members of our group, Sachin Mali, Ganesh, Susheel, Rajkumar, Veeresh, Anindita, Rahi, Rupal, Sachin, Yogesh, Puneeth, Sanjit, Sereena, Vivek, Ranjana and Rajat for their gentle cooperation and help. I especially extend my sincere gratitude to Rajkumar for spending his valuable time to guide me throughout this period to improve the quality of this project work.

I also extend my sincere thanks to Archana for XRD, Swati and Mahesh for MALDI, Nitin for NMR and Anil and Yathish for SEM.

Finally, I would like to acknowledge Prof. K. N. Ganesh for conceiving this institute with great infrastructure and world class facilities that everyone in this institute is privileged with.

This project has been a great platform for learning and self-development. I am very delightful for having a substantial exposure to the fascinating area of scientific research.

CONTENTS

Abbreviations

Aib/U = 2-Aminoisobutyric acid

Bn = Benzyl

BnBr = Benzyl bromide

Boc = *tert*-Butoxycarbonyl

$(Boc)_2O$ = Di-*tert*-butyl-dicarbonate (Boc anhydride)

$CHCl_3$ = Chloroform

DCC = N,N'-Dicyclohexylcarbodiimide

DCM = Dichloromethane

DIPEA = Diisoproylethyl amine

DMF = N,N'-Dimethyl formamide

EDC.HCl = 1-(3-Dimethylaminopropyl)-3-ethylcarbodiimide hydrochloride

EtOAc = Ethyl Acetate

EtOH = Ethanol

HOAt = 1-Hydroxy-7-azabenzotriazole

HOBt = 1-Hydroxybenzotriazole

IBX = 2-iodoxybenzoic acid

Leu = Leucine

MeOH = Methanol

TFA = Trifluoro acetic acid

THF = Tetrahydrofuran

Val = Valine

Abstract

Metals play a crucial role in the structure and functions of various proteins. The metal containing active sites of metalloproteins are responsible for important biological processes such as photosynthesis, oxygen transport and storage, respiration and nitrogen fixation. In addition, metals also play an important role in the amyloidogenesis. Inspired by these fascinating properties, chemists have been trying to mimic naturally occurring metalloproteins by synthesizing artificial peptides attached with natural or non-natural metal-binding ligands. Over the past few decades, this strategy has emerged as an important field in the area of supramolecular chemistry and have contributed several supramolecular architectures with potential applications. The design of such novel architectures from peptides requires deep understanding on their structural properties, assembly behaviors and dynamic nature. Motivated by the diverse functions of metallopeptides and proteins, we sought to investigate whether the metals can be used to drive the ordered supramolecular assemblies in hybrid peptide foldamers. Herein, we are presenting the studies on the metal driven supramolecular assembly of peptide foldamers exhibiting diverse structural and assembly properties. The designed tripeptide β sheets with 3-pyridyl ligands at their both termini displayed remarkable supramolecular metallogel upon Ag(I) coordination polymerization. Replacing 3-pyridyl ligands with 4-pyridyl ligands in the same sequence resulted in the formation of Cu(II) metallogel. In contrast, on replacing leucine residue with γ-leucine in these α-peptide sequence resulted in a complete structural transformation from β sheets to 12-helices, as evident from X-ray diffraction analysis. Surprisingly, both these helical peptides self-assembled to form stable metallo-foldamer-gels. In sharp contrast to this observation, the coordination-driven self-assembly of a more stable helical foldamer, designed by incorporating the helix inducer amino acid Aib in its sequence, did not lead to metallogels. However, it produced X-ray quality single crystals and the structural analysis of this complex revealed that the helical structure of the peptide is retained in the complex. From these observations, we hypothesize that the formation of metallogels from helical foldamer ligands may arise from their coordination driven unfolding.

1) INTRODUCTION

Proteins, the heteropolymers made up of amino acids are the most abundant biopolymers found in living systems and play crucial roles in various biochemical processes of life. Their unique ability for adopting various rigid and definite three-dimensional conformations is the key factor for their complex functions. These functional quaternary and tertiary structures of proteins are constructed from a limited number of secondary structural elements, such as β -sheets, helices, turns and loosely structured loops.

Metal ions are often associated with proteins and enzymes and are known to play important roles in structural, regulatory and enzymatic activity.[1] In nature, nearly one-third of proteins require metal ions as cofactors for their biological functions. Hence, mimicking naturally occurring metalloproteins by means of synthesizing artificial peptides with incorporated natural or non-natural metal-binding sites is a field of great interest. It is also known that, often, coordination of metal ions to the peptide can induce conformational changes in the peptide, resulting in changes in their properties.[2] For, instance a transition from α-helix to β-sheet has been observed in the β-amyloid peptides after coordination with metals.[3] In addition, coordination of metals are also known to drive the self-assembly of peptides through metal-ligand interactions and the resulting supramolecular structures can be conformationally and functionally rather different from the original peptides.[4] These unique properties of metal driven supramolecular assembly provide an excellent platform for the construction of stable macroscopic structures with interesting properties.

In the past few decades, the field of supramolecular chemistry has achieved substantial advances in creating novel materials such as, metal–organic frameworks (MOFs),[5] coordination metal–organic polymers and gels,[6] supramolecular cages etc.[7] and these are shown to have potential applications in several areas such as catalysis,[8] sensing[9] and molecular recognition.[7] Peptides themselves are known to exhibit remarkable self-assembly properties and are shown to adopt diverse nanoarchitectures such as micelles, ribbons, tapes, fibers, vesicles, and tubes.[10-15] In this context, exploration of peptides as ligands may offer a new dimension in the construction of diverse supramolecular assemblies, since they can provide an enormous chemical space in terms of functional groups, polarity and charge.

Chmielewski and co-workers synthesized artificial collagen-based peptides exhibiting a triple helix formation and conducted extensive studies on the behavior of these peptides in presence of metals. These peptides were shown to self-assemble into discs, spherical shells or fibrous structures.[16] Recently, the same group reported a facile strategy for accessing the crystal structure of coiled coil peptides through metal-driven hierarchical self-assembly, which is otherwise very hard to achieve.[17] Studies conducted by Horne and colleagues showed the metal directed assembly of coiled coil peptides into well-defined supramolecular nets and frame works.[18] Fujita et al. have constructed a metal driven protein like channel[19] as well as peptide [4] catenane[20] from the coordination driven assembly of short peptides. Metal driven self-assembly of peptide ligands are also shown to form stable metallogels with catalytic properties.[21]

The particular aim of this project is to understand the structural properties and metal driven supramolecular assembly of peptide foldamers. For this purpose, we have designed both β-sheets and hybrid helices incorporated with pyridyl ligands at N- and C- termini of the peptides. We have chosen to include both 3-pyridyl and 4-pyridyl ligands as the metal binding ligands, owing to their different affinities to different metals. The sequences of the designed peptides under investigation are shown in Figure 1. The peptides **P1** and **P3**, composed of Val-Leu-Val along with 3-pyridyl and 4-pyridyl groups respectively, at their C- and N-terminus were designed as β-sheet promoting peptides. Replacement of the middle leucine residues in these sequences with γ-leucine gave rise to the α/γ4-hybrid peptide helices **P2** and **P4**, respectively. The design of these helical peptides is inspired by the previous work on α/γ4-hybrid peptides from our group.[22] The, α/γ4-hybrid peptide **P5**, bis(3-pyridyl) terminated Aib-γLeu-Leu, was designed as a control helical peptide. Aib is known to induce either 3_{10} or α-helix in peptides. Hence we anticipate that **P5** can adopt the helical structure with better stability than **P2** and **P4**. Further details on the synthesis, structural analysis and supramolecular assembly of these peptides are explained in the following sections.

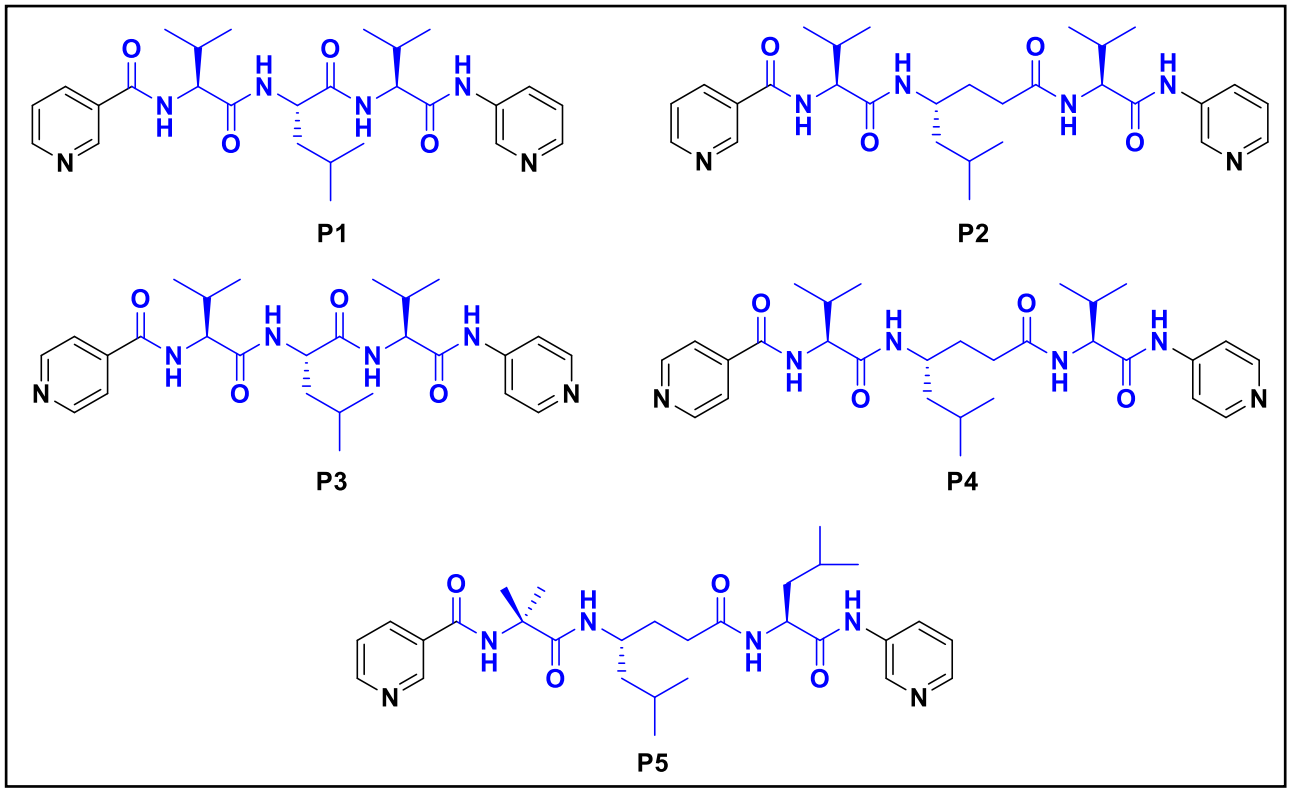

Figure 1: Chemical structures of the peptides designed for this study

2) METHODS

2.1) Experimental Section:

All amino acids, EDC.HCl, HOAt, $AgBF_4$, $CuCl_2.3H_2O$ and NMR solvents were purchased from Aldrich. THF, DCM, DMF, Methanol, Ethanol, Chloroform, EtOAc and Hexane were purchased from Merck. 3-aminopyridine, 4-aminopyridine, Nicotinic acid, Isonicotinic acid, di-tert-butyl dicarbonate, TFA, Benzyl Bromide, Ethyl Bromoacetate, Triphenyl Phosphine, Oxone, DIPEA, $NaBH_4$, DCC and HOBt were obtained from spectrochem and used without further purification. Column chromatography was performed on Merck silica gel (120–200 mesh). The ^{1}H spectra were recorded on *Jeol* 400 MHz (or 100 MHz for ^{13}C) / Bruker 400 MHz (or 100 MHz for ^{13}C) spectrometers using residual solvent signals as an internal reference (DMSO-D6 ^{1}H-2.50 ppm, ^{13}C-39.5 ppm). The chemical shifts (δ) are reported in ppm and coupling constants (J) in Hz.

2.1.1) Procedure for the Synthesis of *N*- Boc-protected γ-leucine:

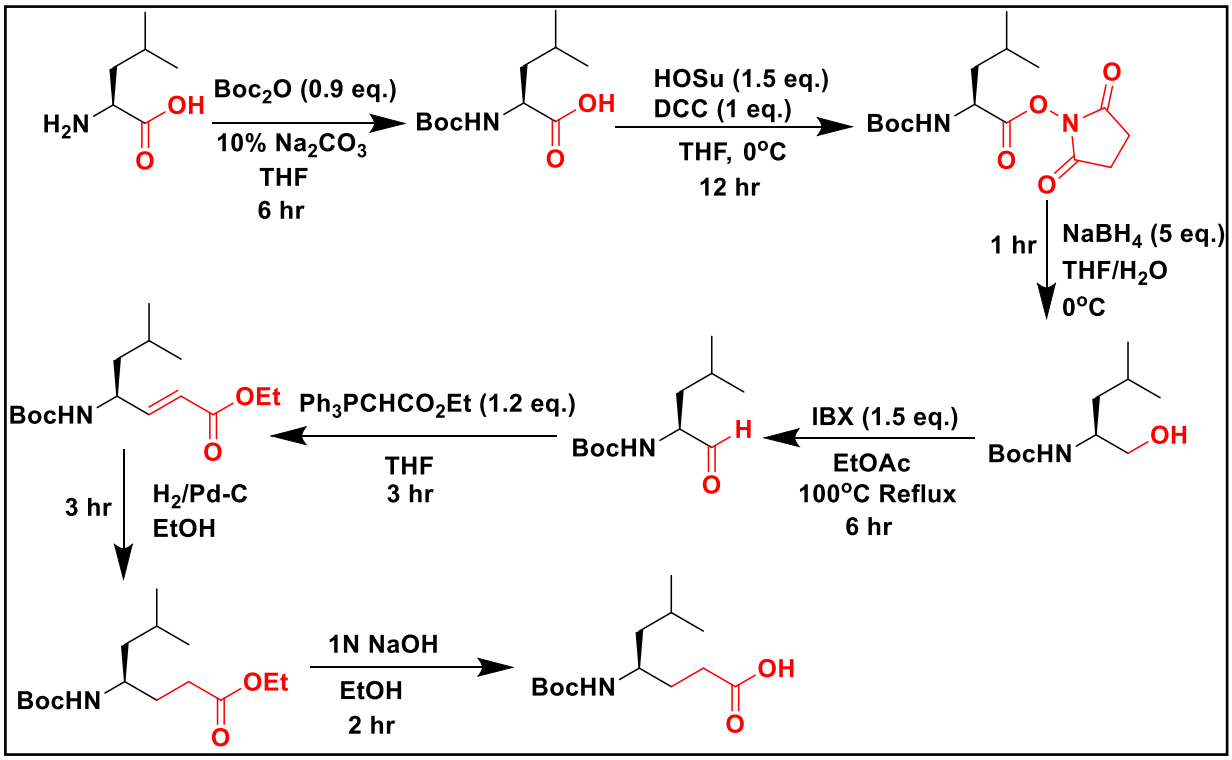

Scheme 1: Procedure for the synthesis of *N*- Boc-protected γ-leucine

The synthesis of *N*- Boc-protected γ-leucine starting from α-leucine was carried out according to the above-mentioned procedure, which is previously reported.[23]

2.1.2) Synthetic Procedure for P1:

N-Boc protected valine (20 mmol, 4.34 g) was dissolved in 20 mL of DMF. To this anhydrous K_2CO_3 (30 mmol, 5.8 g) was added under constant stirring. The reaction mixture was capped with N_2 balloon followed by the addition of benzyl bromide (20 mmol, 2.4 mL). The progress of the reaction was monitored using TLC. Upon completion, the reaction mixture was diluted with 200 mL EtOAc and was washed with water (150 mL X 2) and brine (150 mL X 1) and the collected organic layer was dried over anhydrous Na_2SO_4 and was evaporated to dryness to get a viscous liquid, C1 (Yield- 5.90 g, 96%).

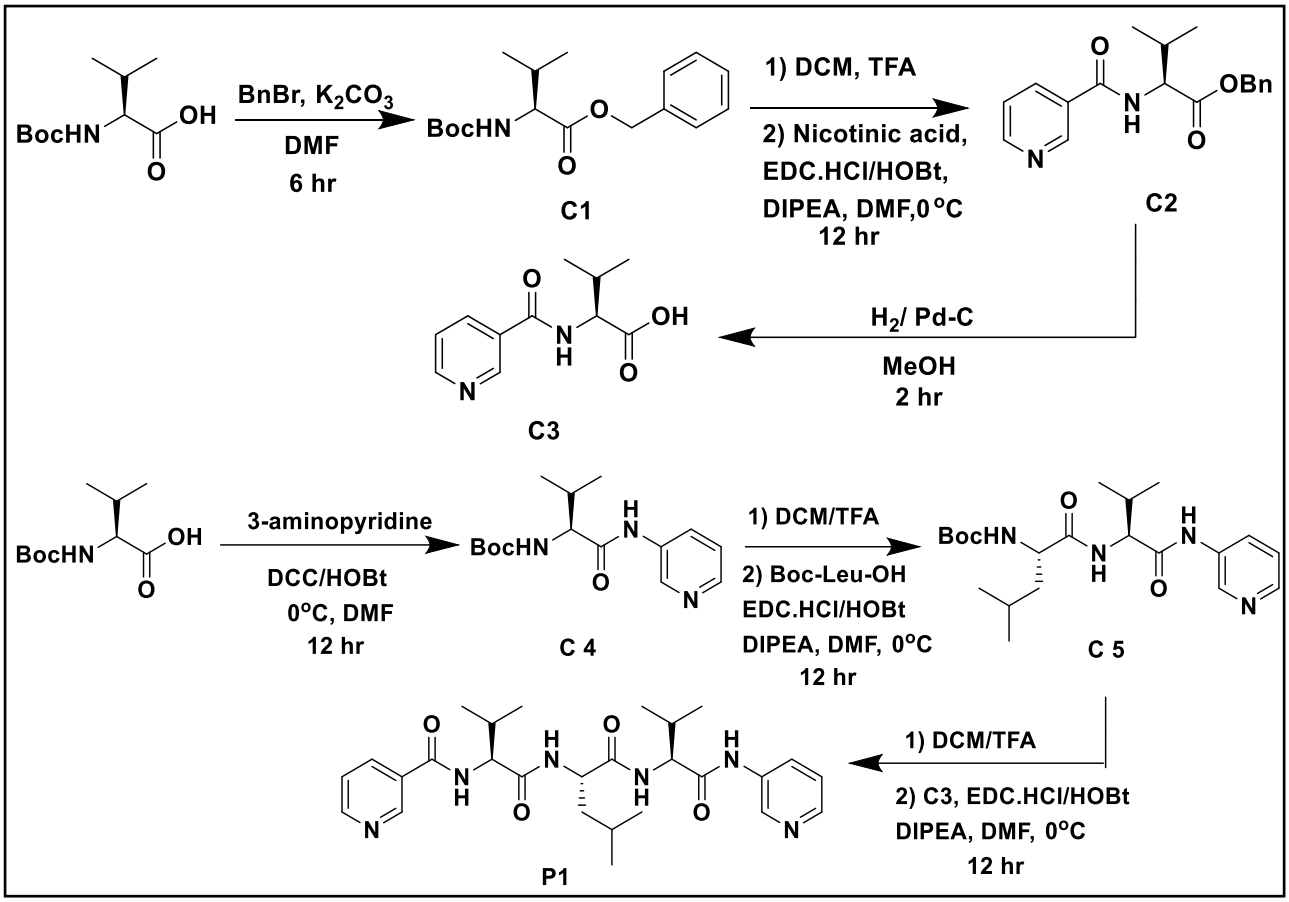

Scheme 2: Synthetic route for P1

C1 (9.2 mmol, 2.83 g) was further subjected to Boc-deprotection using 50% TFA in DCM (9 mL TFA in 9 mL DCM). Upon completion of the reaction, the reaction mixture was evaporated several times with DCM to remove the residual TFA. The resulting TFA salt of the amine was dissolved in 2 mL DMF and was quenched with 4 equivalents of DIPEA (6.4 mL) to get the amine cocktail of C1.

To the free amine of C1, nicotinic acid (9 mmol, 2.80 g) dissolved in a mixture of 6 mL of DMF and one equivalent (1.6 mL) of DIPEA was added. The reaction mixture was then cooled down to 0°C using an ice bath in N_2 atmosphere. To this, EDC.HCl (9 mmol, 1.73 g) and HOBt (9 mmol, 1.22 g) were added and the reaction mixture was stirred overnight. Upon completion, the reaction mixture was diluted with 150 mL of EtOAc and was washed with water (100 mL X 1), 10% Na_2CO_3 solution (100 mL X 3) and finally with brine (100 mL X 1). The organic layer was dried over anhydrous Na_2SO_4 and concentrated

under reduced pressure to give a crude oily product which was then subjected to column chromatography to get pure oily liquid, C2 (Yield- 2.39 g, 85%).

The C2 (7.36 mmol, 2.30 g) was then subjected to catalytic hydrogenation to remove benzyl group using 20 weight % of 10% Pd on carbon (0.46 g) catalyst in dry MeOH. After completion, the reaction mixture was diluted with 50 mL of EtOAc and filtered through a bed of celite filled in a sintered funnel. The filtrate was then collected and concentrated under reduced pressure to get a yellowish white powder, C3 (Yield- 1.59 g, 97%).

The amide C4 was synthesized starting from Boc-Val-OH. Briefly, the *N*-Boc protected valine (20 mmol, 4.34 g) was dissolved in 20 mL of DMF and cooled to 0 ^{o}C under N_2 atmosphere. To this, DCC (20 mmol, 4.14 g) and HOBt (20 mmol, 2.72 g) were added and the reaction mixture was stirred for 10 minutes. This was followed by the addition of 3-aminopyridine (24 mmol, 2.26 g). The reaction mixture was stirred for overnight and the progress was monitored by TLC. Upon completion, the reaction mixture was diluted with 200 mL EtOAc and was filtered through a sintered funnel filled with a bed of celite. The filtrate was washed with water (150 mL X 1), 10% Na_2CO_3 solution (150 mL X 3) and finally with brine (150 mL X 1). The organic layer was dried over anhydrous Na_2SO_4 and concentrated under reduced pressure to give a crude powder which was then purified by column chromatography to get a white crystalline product C4 (Yield- 5.22 g, 89%).

The C4 (8.2 mmol, 2.41 g) was then subjected to Boc-deprotection using 50% TFA in DCM (8 mL TFA in 8 mL DCM). Upon completion, the reaction mixture was evaporated several times with DCM to remove the residual TFA. The resulting TFA salt of the amine was dissolved in 2 mL DMF and was quenched with 5 equivalents of DIPEA (7.1 mL) to get the amine cocktail of C4.

N-Boc protected leucine (8 mmol, 1.85 g) was dissolved in 6 mL of DMF. The reaction mixture was then cooled down to 0^{o}C using an ice bath in N_2 atmosphere. To this, EDC.HCl (8 mmol, 1.54 g) and HOBt (8 mmol, 1.09 g) were added and the reaction mixture was stirred for 10 minutes. This was followed by the addition previously prepared amine cocktail of C4. The reaction mixture was stirred for overnight. Upon completion, the reaction mixture was diluted with 150 mL of EtOAc and was washed with water (100

mL X 1), 10% Na_2CO_3 solution (100 mL X 3) and finally with brine (100 mL X 1). The organic layer was dried over anhydrous Na_2SO_4 and concentrated under reduced pressure to give a crude powder which was then purified by column chromatography yielding a white powder, C5 (Yield- 2.80 g, 86%).

The C5 (6.8 mmol, 2.77g) was then subjected to Boc-deprotection using 50% TFA in DCM (7 mL TFA in 7 mL DCM). Upon completion, the reaction mixture was evaporated several times with DCM to remove the residual TFA. The resulting TFA salt of the amine was dissolved in 2mL DMF and was quenched with 5 equivalents of DIPEA (5.9 mL) to get the amine cocktail of C5.

The amino acid C3 (6.5 mmol, 1.45 g) was dissolved in 4 mL of DMF. The reaction mixture was then cooled down to 0^oC using an ice bath in N_2 atmosphere. To this, EDC.HCl (6 mmol, 1.16 g) and HOBt (6 mmol, 1.09g) was added and the reaction mixture was stirred for 10 minutes. This was followed by the addition previously prepared free amine of C5. The reaction mixture was stirred overnight. Upon completion, the reaction mixture was diluted with 150 mL of EtOAc and was washed with water (100 mL X 1), 10% Na_2CO_3 solution (100 mL X 3) and finally with brine (100 mL X 1). The organic layer was dried over anhydrous Na_2SO_4 and concentrated under reduced pressure to give a crude peptide **P1**, which was then purified by column chromatography (Yield- 2.76 g, 83%).

2.1.3) Synthetic Procedure for P2:

Previously prepared C4 (6.2 mmol, 1.82 g) was subjected to Boc-deprotection using 50% TFA in DCM (6 mL TFA in 6 mL DCM). Upon completion, the reaction mixture was evaporated several times with DCM to remove the residual TFA. Resulting TFA salt of the amine was dissolved in 2 mL DMF and was quenched with 5 equivalents of DIPEA (5.3 mL) to get the amine cocktail of C4.

N-Boc protected γ-leucine (6 mmol, 1.56 g) was dissolved in a 4 mL of DMF and was cooled down to 0 ^oC using an ice bath in N_2 atmosphere. To this, EDC.HCl (6 mmol, 1.16 g) and HOBt (6 mmol, 0.82 g) were added and the reaction mixture was stirred for 10 minutes. This was followed by the addition of previously prepared amine cocktail of C4. The reaction mixture was stirred for overnight and reaction progress was monitored using TLC. Upon completion, the reaction mixture was diluted with 150 mL of EtOAc and

was washed with water (100 mL X 1), 10% Na_2CO_3 solution (100 mL X 3) and finally with brine (100 mL X 1). The organic layer was dried over anhydrous Na_2SO_4 and concentrated under reduced pressure to give a crude solid which was then subjected to column chromatography to get a pure crystalline powder, C6 (Yield- 2.17 g, 83%).

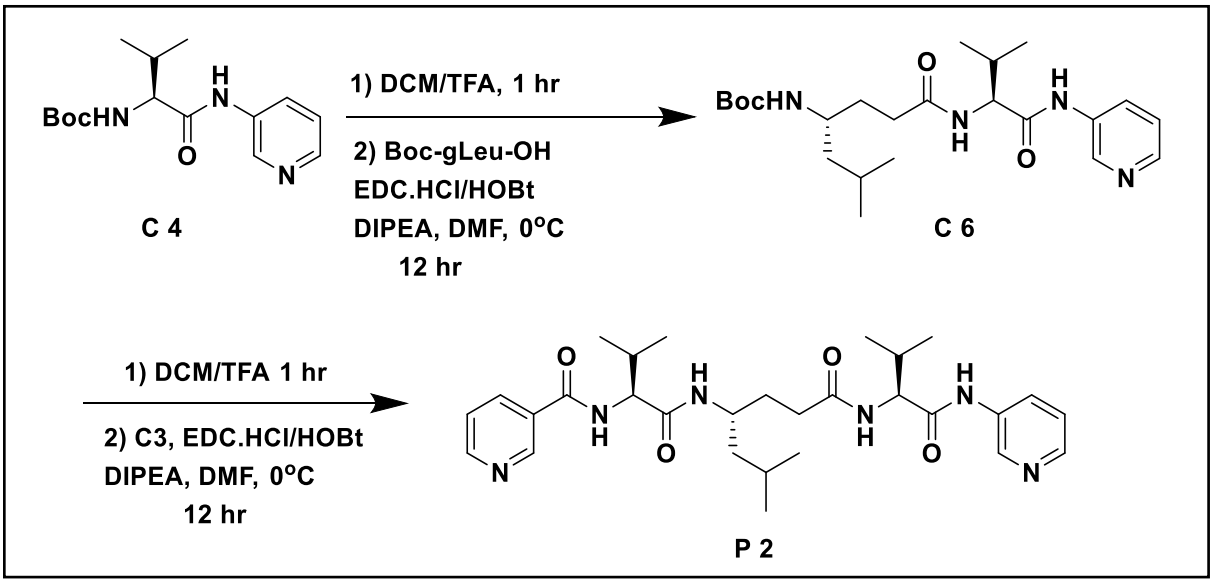

Scheme 3: Synthetic route for P2

C6 (4.8 mmol, 2.09 g) was then subjected to Boc-deprotection using 50% TFA in DCM (5 mL TFA in 5 mL DCM). Upon completion, the reaction mixture was evaporated several times with DCM to remove the residual TFA. The resulting TFA salt of the amine was dissolved in 2 mL of DMF and was quenched with 5 equivalents of DIPEA (4.2 mL) to get the amine cocktail of C6.

Previously prepared C3 (4.8 mmol, 1.07 g) was dissolved in 3 mL of DMF and the reaction mixture was then cooled down to 0 °C using an ice bath in N_2 atmosphere. To this, EDC.HCl (4.8 mmol, 0.93 g) and HOBt (4.8 mmol, 0.65 g) were added and the reaction mixture was stirred for 10 minutes. This was followed by the addition of previously prepared amine cocktail of C6. The reaction mixture was stirred for overnight. Upon completion, the reaction mixture was diluted with 150 mL of EtOAc and was washed with water (100 mL X 1), 10% Na_2CO_3 solution (100 mL X 3) and finally with brine solution (100 mL X 1). The organic layer was dried over anhydrous Na_2SO_4 and concentrated

under reduced pressure to give a crude powder which was then purified by column chromatography yielding a white powder, **P2** (Yield- 2.23 g, 86%).

2.1.4) Synthetic Procedure for P3:

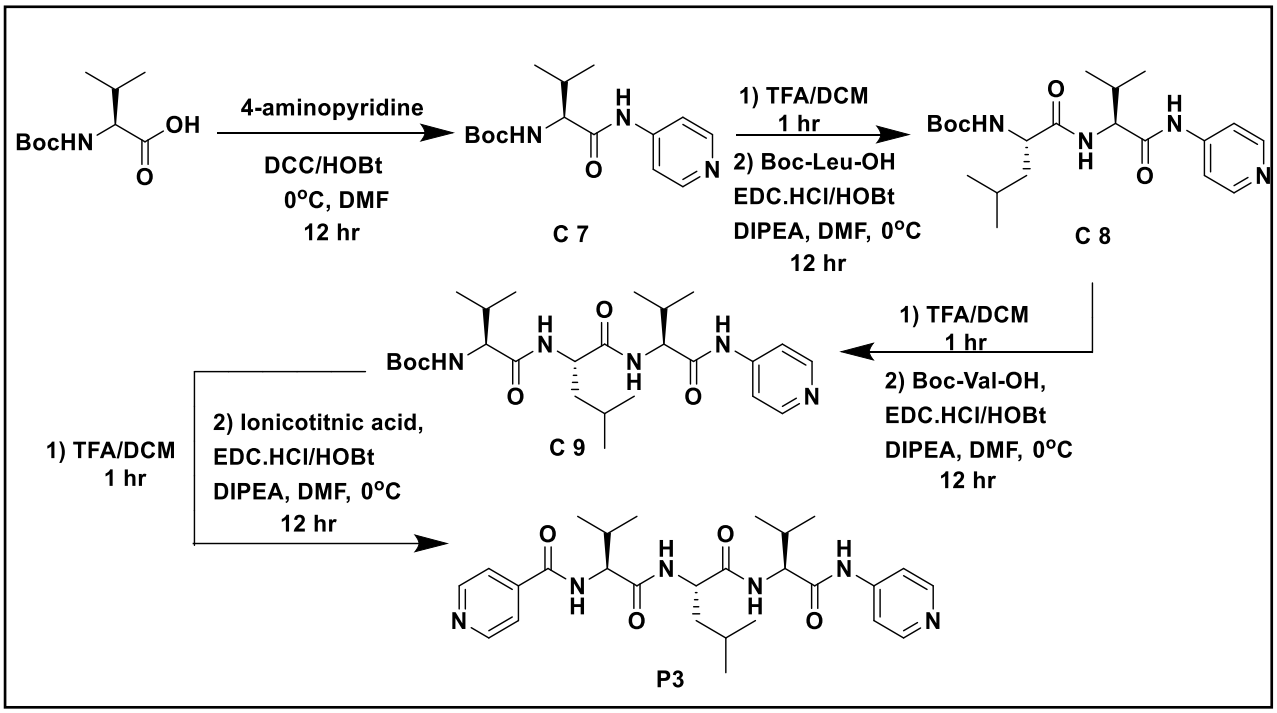

Scheme 4: Synthetic route for the peptide P3

N-Boc protected valine (20 mmol, 4.34 g) was dissolved in 20 mL of DMF and was cooled down to 0°C under N_2 atmosphere. To this, DCC (20 mmol, 4.14 g) and HOBt (20 mmol, 2.72 g) were added and the reaction mixture was stirred for 10 minutes. This was followed by the addition of 4-aminopyridine (24 mmol, 2.26 g). The reaction mixture was stirred for overnight and the progress was monitored by TLC. Upon completion, the reaction mixture was diluted with 200 mL EtOAc and was filtered through a sintered funnel filled with a bed of celite. The filtrate was washed with water (150 mL X 1), 10% Na_2CO_3 solution (150 mL X 3) and finally with brine solution (150 mL X 1). The organic layer was dried over anhydrous Na_2SO_4 and concentrated under reduced pressure to give a crude powder which was then purified by column chromatography to get a white crystalline product C7 (Yield- 5.05 g, 86%).

The amide C7 (8.2 mmol, 2.41 g) was then subjected to Boc-deprotection using 50% TFA in DCM (8 mL TFA in 8 mL DCM). Upon completion, the reaction mixture was evaporated several times with DCM to remove the residual TFA. The resulting TFA salt of the amine was dissolved in 2mL DMF and was quenched with 5 equivalents of DIPEA (7 mL) to get the free amine of C7.

N-Boc protected leucine (8 mmol, 1.85 g) was dissolved in 6 mL of DMF. The reaction mixture was then cooled down to 0^{o}C using an ice bath in N_2 atmosphere. To this, EDC.HCl (8 mmol, 1.54 g) and HOBt (8 mmol, 1.09 g) were added and the reaction mixture was stirred for 10 minutes. This was followed by the addition previously prepared amine cocktail of C7. The reaction mixture was stirred overnight. Upon completion, the reaction mixture was diluted with 150 mL of EtOAc and was washed with water (100 mL X 1), 10% Na_2CO_3 (100 mL X 3) and finally with brine (100 mL X 1). The organic layer was dried over anhydrous Na_2SO_4 and concentrated under reduced pressure to give a crude dipeptide C8 which was then purified by column chromatography (Yield- 2.72 g, 83%).

The dipeptide C8 (6.15 mmol, 2.50 g) was then subjected to Boc-deprotection using 50% TFA in DCM (6 mL TFA in 6 mL DCM). Upon completion, the reaction mixture was evaporated several times with DCM to remove the residual TFA. The resulting TFA salt of the amine was dissolved in 1.5 mL DMF and was quenched with 5 equivalents of DIPEA (5.3 mL) to get free amine of C8.

N-Boc protected Valine (6 mmol, 1.31 g) was dissolved in 4 mL of DMF. The reaction mixture was then cooled down to 0 ^{o}C using an ice bath in N_2 atmosphere. To this, EDC.HCl (6 mmol, 1.16 g) and HOBt (6 mmol, 0.82 g) were added and the reaction mixture was stirred for 10 minutes. This was followed by the addition previously prepared amine of C8. The reaction mixture was stirred overnight. Upon completion, the reaction mixture was diluted with 150 mL of EtOAc and was washed with water (100 mL X 1), 10% Na_2CO_3 (100 mL X 3) and finally with brine (100 mL X 1). The organic layer was dried over anhydrous Na_2SO_4 and concentrated under reduced pressure to give a crude peptide C9, which was then purified by column chromatography (Yield- 2.55 g, 84%).

The tripeptide C9 (4.75 mmol, 2.40 g) was then subjected to Boc-deprotection using 50% TFA in DCM (5 mL TFA in 5 mL DCM). Upon completion, the reaction mixture

was evaporated several times with DCM to remove the residual TFA. The resulting TFA salt of the amine was dissolved in 1.5 mL DMF and was quenched with 5 equivalents of DIPEA (3.3 mL) to get the amine of C9.

To this free amine, isonicotinic acid (4.7 mmol, 0.58 g) dissolved in a mixture of 2.5 mL of DMF and one equivalent of DIPEA (0.8 mL) was added. The reaction mixture was then cooled to 0 ^{o}C using an ice bath in N_2 atmosphere. To this, EDC.HCl (4.7 mmol, 0.91 g) and HOBt (4.7 mmol, 0.64 g) were added and the reaction mixture was stirred overnight. Upon completion, the reaction mixture was diluted with 150 mL of EtOAc and was washed with water (100 mL X 1), 10% Na_2CO_3 solution (100 mL X 3) and finally with brine solution (100 mL X 1). The organic layer was dried over anhydrous Na_2SO_4 and concentrated under reduced pressure to give the crude peptide which was then subjected to the column chromatography to get pure peptide **P3** (Yield- 2.02 g, 84%).

2.1.5) Synthetic Procedure for P4:

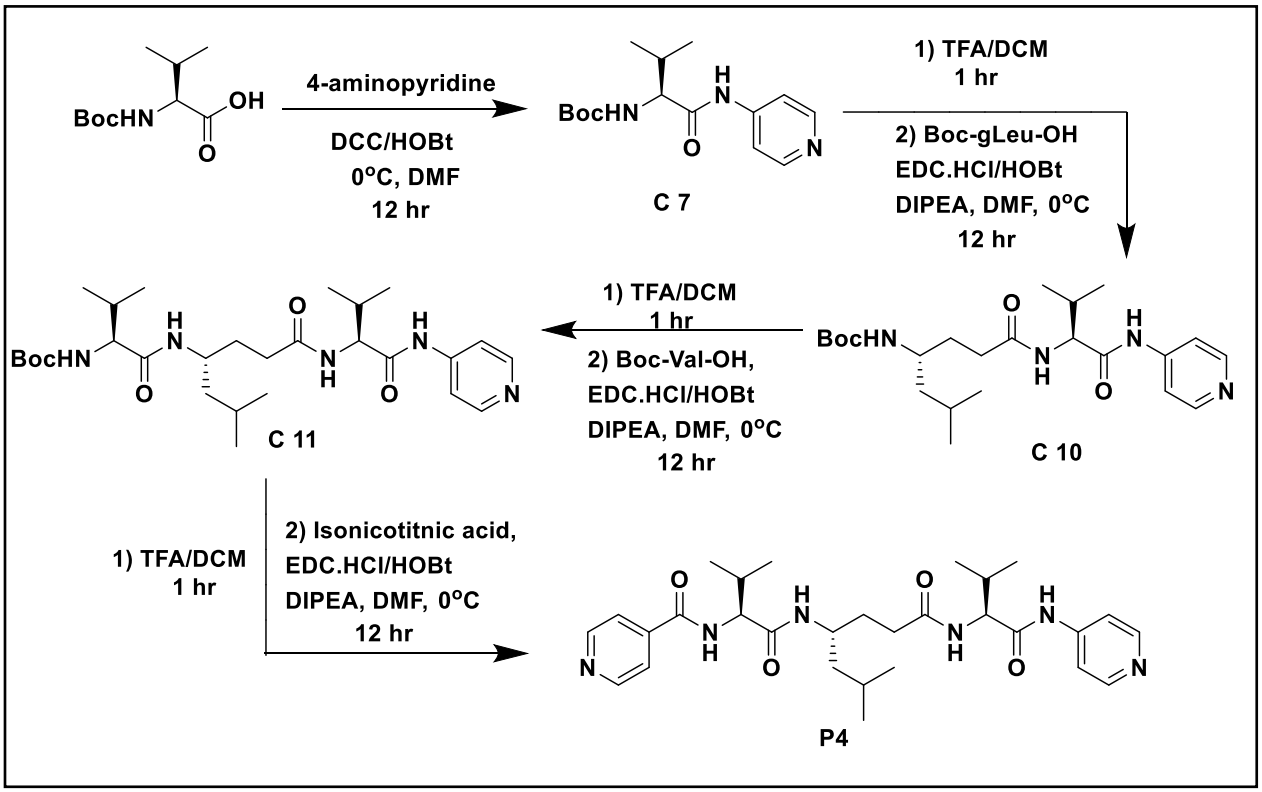

Scheme 5: Synthetic route for P4

Previously prepared C7 (5.2 mmol, 1.53 g) was subjected to Boc-deprotection using 50% TFA in DCM (5 mL TFA in 5 mL DCM). Upon completion, the reaction mixture was evaporated several times with DCM to remove the residual TFA. The resulting TFA salt of amine was dissolved in 2 mL DMF and was quenched with 5 equivalents of DIPEA (4.5 mL) to get the free amine of C7.

To this free amine, *N*-Boc protected γ-leucine (5 mmol, 1.30 g) dissolved in 3 mL of DMF was added. The reaction mixture was then cooled to 0 ^{o}C using an ice bath in N_2 atmosphere. To this, EDC.HCl (5 mmol, 0.96 g) and HOBt (5 mmol, 0.68 g) were added and the reaction mixture was stirred overnight. Upon completion, the reaction mixture was diluted with 150 mL of EtOAc and was washed with water (100 mL X 1), 10% Na_2CO_3 solution (100 mL X 3) and finally with brine (100 mL X 1). The organic layer was dried over anhydrous Na_2SO_4 and concentrated under reduced pressure to give a crude peptide which was then purified by column chromatography to get pure peptide C10 (Yield- 1.85 g, 85%).

The peptide C10 (4.14 mmol, 1.80 g) was then subjected to Boc-deprotection using 50% TFA in DCM (4 mL TFA in 4 mL DCM). Upon completion, the reaction mixture was evaporated several times with DCM to remove the residual TFA. The resulting TFA salt of the amine was dissolved in 1 mL DMF and was quenched with 5 equivalents of DIPEA (3.6 mL) to get free amine of C10.

To this free amine, the *N*-Boc protected valine (4.1 mmol, 0.89 g) dissolved in 2.5 mL of DMF was added. The reaction mixture was then cooled to 0^{o}C using an ice bath in N_2 atmosphere. To this, EDC.HCl (4.1 mmol, 0.79 g) and HOBt (4.1 mmol, 0.56 g) were added and the reaction mixture was stirred overnight. Upon completion, the reaction mixture was diluted with 150 mL of EtOAc and was washed with water (100 mL X 1), 10% Na_2CO_3 solution (100 mL X 3) and finally with brine solution (100 mL X 1). The organic layer was dried over anhydrous Na_2SO_4 and concentrated under reduced pressure to give a crude peptide which was then purified by column chromatography to get pure C11 (Yield- 1.75 g, 80%).

The C11 (3.19 mmol, 1.71 g) was further subjected to Boc-deprotection using 50% TFA in DCM (3 mL TFA in 3 mL DCM). Upon completion, the reaction mixture was evaporated several times with DCM to remove the residual TFA. The resulting TFA salt

of the amine was dissolved in 1 mL DMF and was quenched with 4 equivalents of DIPEA (2.2 mL) to get the free amine of C11.

To this free amine, isonicotinic acid (3.1 mmol, 0.385 g) dissolved in a mixture of 2 mL of DMF and one equivalent (0.54 mL) of DIPEA was added. The reaction mixture was then cooled down to 0^{o}C using an ice bath in N_2 atmosphere. To this, EDC.HCl (3.1 mmol, 0.56 g) and HOBt (3.1 mmol, 0.42 g) were added and the reaction mixture was stirred overnight. Upon completion, the reaction mixture was diluted with 150 mL of EtOAc and was washed with water (100 mL X 1), 10% Na_2CO_3 solution (100 mL X 3) and finally with brine solution (100 mL X 1). The organic layer was dried over anhydrous Na_2SO_4 and concentrated under reduced pressure to give a crude peptide which was then subjected to column chromatography to get the pure peptide, **P4** (Yield- 1.39 g, 83%).

2.1.6) Synthetic Procedure for P5:

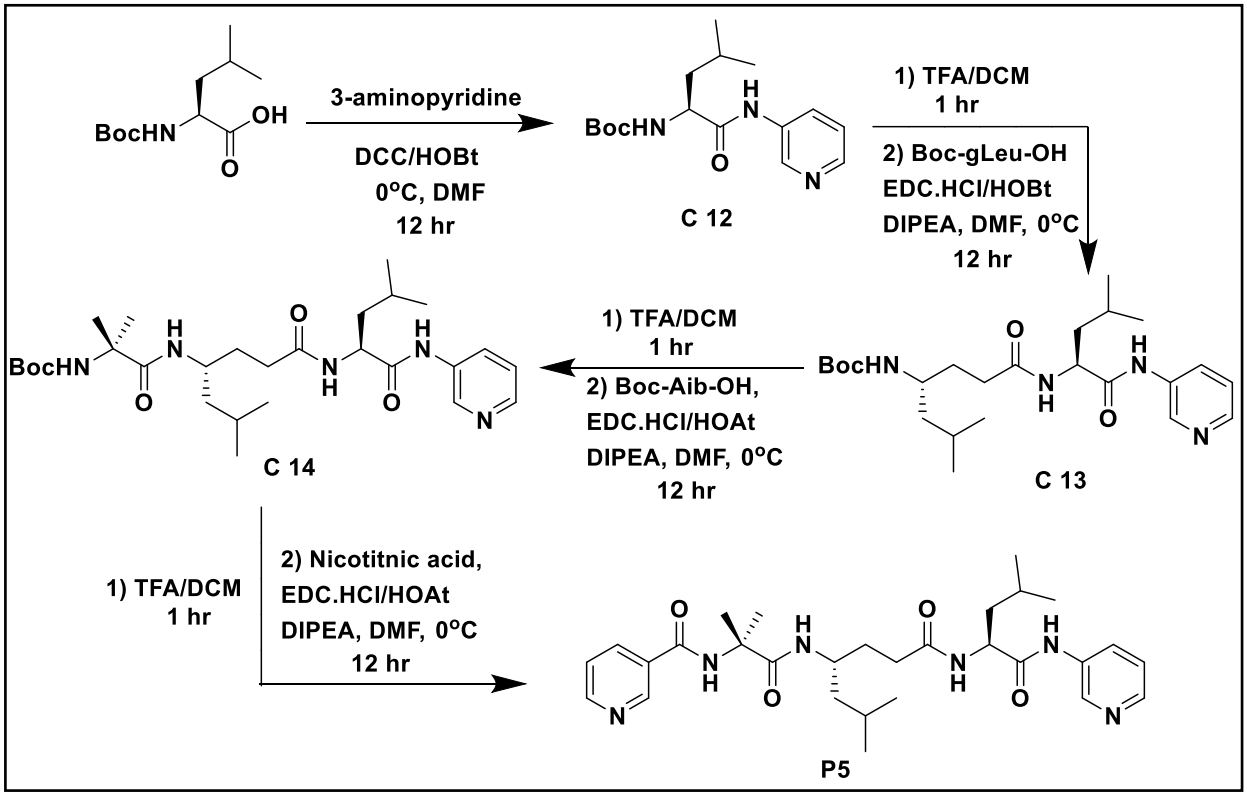

Scheme 6: Synthetic route for P5

N-Boc protected leucine (10 mmol, 2.31 g) was dissolved in 10 mL of DMF and was cooled down to 0^{o}C under N_2 atmosphere. To this, DCC (10 mmol, 2.07 g) and HOBt (10 mmol, 1.36 g) were added and the reaction mixture was stirred for 10 minutes. This was followed by the addition of 4-aminopyridine (12 mmol, 1.13 g). The reaction mixture was stirred for overnight and the progress was monitored by TLC. Upon completion, the reaction mixture was diluted with 150 mL EtOAc and was filtered through a sintered funnel filled with a bed of celite. The filtrate was washed with water (100 mL X 1), 10% Na_2CO_3 (100 mL X 3) and finally with brine solution (100 mL X 1). The organic layer was dried over anhydrous Na_2SO_4 and concentrated under reduced pressure to give a crude powder which was then purified by column chromatography to get a white crystalline product C12 (Yield- 2.74 g, 89%).

C12 (5.2 mmol, 1.60 g) was subjected to Boc-deprotection using 50% TFA in DCM (5 mL TFA in 5 mL DCM). Upon completion, the reaction mixture was evaporated several times with DCM to remove the residual TFA. The resulting TFA salt of the amine was dissolved in 2mL DMF and was quenched with 5 equivalents of DIPEA (4.5 mL) to get the free amine of C12.

To this free amine, *N*-Boc protected γ-leucine (5 mmol, 1.30 g) dissolved in 3 mL of DMF was added. The reaction mixture was then cooled down to 0^{o}C using an ice bath in N_2 atmosphere. To this, EDC.HCl (5 mmol, 0.96 g) and HOBt (5 mmol, 0.68 g) were added and the reaction mixture was stirred overnight. Upon completion, the reaction mixture was diluted with 150 mL of EtOAc and was washed with water (100 mL X 1), 10% Na_2CO_3 solution (100 mL X 3) and finally with brine solution (100 mL X 1). The organic layer was dried over anhydrous Na_2SO_4 and concentrated under reduced pressure to give a crude peptide which was then purified by column chromatography to get pure C13 (Yield- 1.98 g, 88%).

C13 (4.35 mmol, 1.95 g) was then subjected to Boc-deprotection using 50% TFA in DCM (4 mL TFA in 4 mL DCM). Upon completion, the reaction mixture was evaporated several times with DCM to remove the residual TFA. Resulting TFA salt of the amine was dissolved in 1 mL of DMF and was quenched with 5 equivalents of DIPEA (2.8 mL) to get free amine of C13.

To this free amine, *N*-Boc protected α-aminoisobutyric acid (4.3 mmol, 0.88 g) dissolved in 2.5 mL of DMF was added. The reaction mixture was then cooled to 0^{o}C using an ice bath in N_2 atmosphere. To this, EDC.HCl (4.3 mmol, 0.83 g) and HOAt (4.3 mmol, 0.59 g) were added and the reaction mixture was stirred overnight. Upon completion, the reaction mixture was diluted with 150 mL of EtOAc and was washed with water (100 mL X 1), 10% Na_2CO_3 (100 mL X 3) and finally with brine (100 mL X 1). The organic layer was dried over anhydrous Na_2SO_4 and concentrated under reduced pressure to give a crude peptide which was then purified by column chromatography to get pure C14 (Yield- 1.73 g, 75%).

The peptide C14 (3.19 mmol, 1.70 g) was then subjected to Boc-deprotection using 50% TFA in DCM (3 mL TFA in 3 mL DCM). Upon completion, the reaction mixture was evaporated several times with DCM to remove the residual TFA. The resulting TFA salt of the amine was dissolved in 1 mL DMF and was quenched with 4 equivalents of DIPEA (2.2 mL) to get free amine of C14.

To this free amine, isonicotinic acid (3.15 mmol, 0.39 g) dissolved in a mixture of 2 mL of DMF and one equivalent (0.55 mL) of DIPEA was added. The reaction mixture was then cooled to 0 ^{o}C using an ice bath in N_2 atmosphere. To this, EDC.HCl (3.15 mmol, 0.60 g) and HOAt (3.15 mmol, 0.43 g) were added and the reaction mixture was stirred overnight. Upon completion, the reaction mixture was diluted with 150 mL of EtOAc and washed with water (100 mL X 1), 10% Na_2CO_3 solution (100 mL X 3) and finally with brine solution (100 mL X 1). The organic layer was dried over anhydrous Na_2SO_4 and concentrated under reduced pressure to give a crude powder which was then subjected to column chromatography to get the pure peptide, **P5** (Yield- 1.27 g, 75%).

2.2) Spectroscopic Data

2.2.1) P1

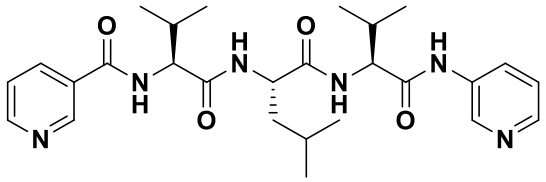

^{1}H NMR (400 MHz, DMSO-D6) δ 10.26 (s, 1H), 8.97 (d, *J* = 1.6 Hz, 1H), 8.69 (d, *J* = 2.4 Hz, 1H), 8.66 (dd, *J* = 4.8, 1.7 Hz, 1H), 8.55 (d, *J* = 8.6 Hz, 1H), 8.22 (dd, *J* = 4.7, 1.5 Hz, 1H), 8.19 – 8.14 (m, 1H), 8.11 (d, *J* = 8.2 Hz, 1H), 8.02 – 7.96 (m, 1H), 7.90 (d, *J* = 8.4 Hz, 1H), 7.49 – 7.43 (m, 1H), 7.30 (dd, *J* = 8.3, 4.7 Hz, 1H), 4.37 (dd, *J* = 14.8, 7.9 Hz, 1H), 4.31 – 4.21 (m, 2H), 2.14 – 2.04 (m, 1H), 1.97 (dq, *J* = 13.7, 7.0 Hz, 1H), 1.58 (dt, *J* = 12.6, 7.3 Hz, 1H), 1.51 – 1.39 (m, 2H), 0.89 – 0.78 (m, 18H).

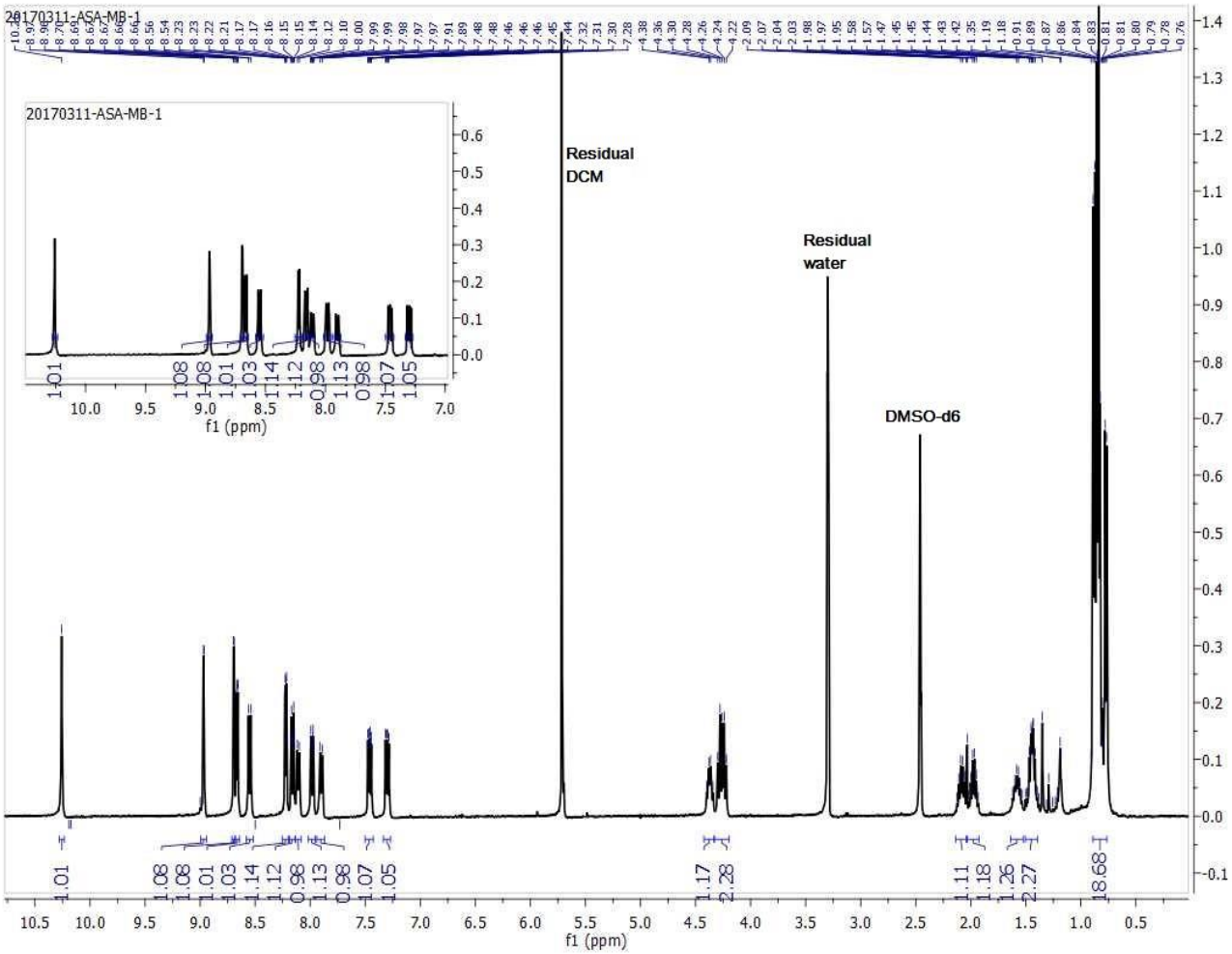

^{13}C NMR (101 MHz, DMSO-d_6) δ 172.45 (s), 171.23 (s), 170.97 (s), 165.65 (s), 152.32 (s), 149.09 (s), 144.82 (s), 141.25 (s), 135.79 (d, J = 13.0 Hz), 130.32 (s), 126.56 (s), 124.12 (s), 123.78 (s), 59.64 (s), 59.04 (s), 51.59 (s), 31.08 (s), 30.46 (s), 26.80 (s), 24.62 (s), 23.50 (s), 22.01 (s), 19.66 (d, J = 19.4 Hz), 19.30 (s), 18.76 (s).

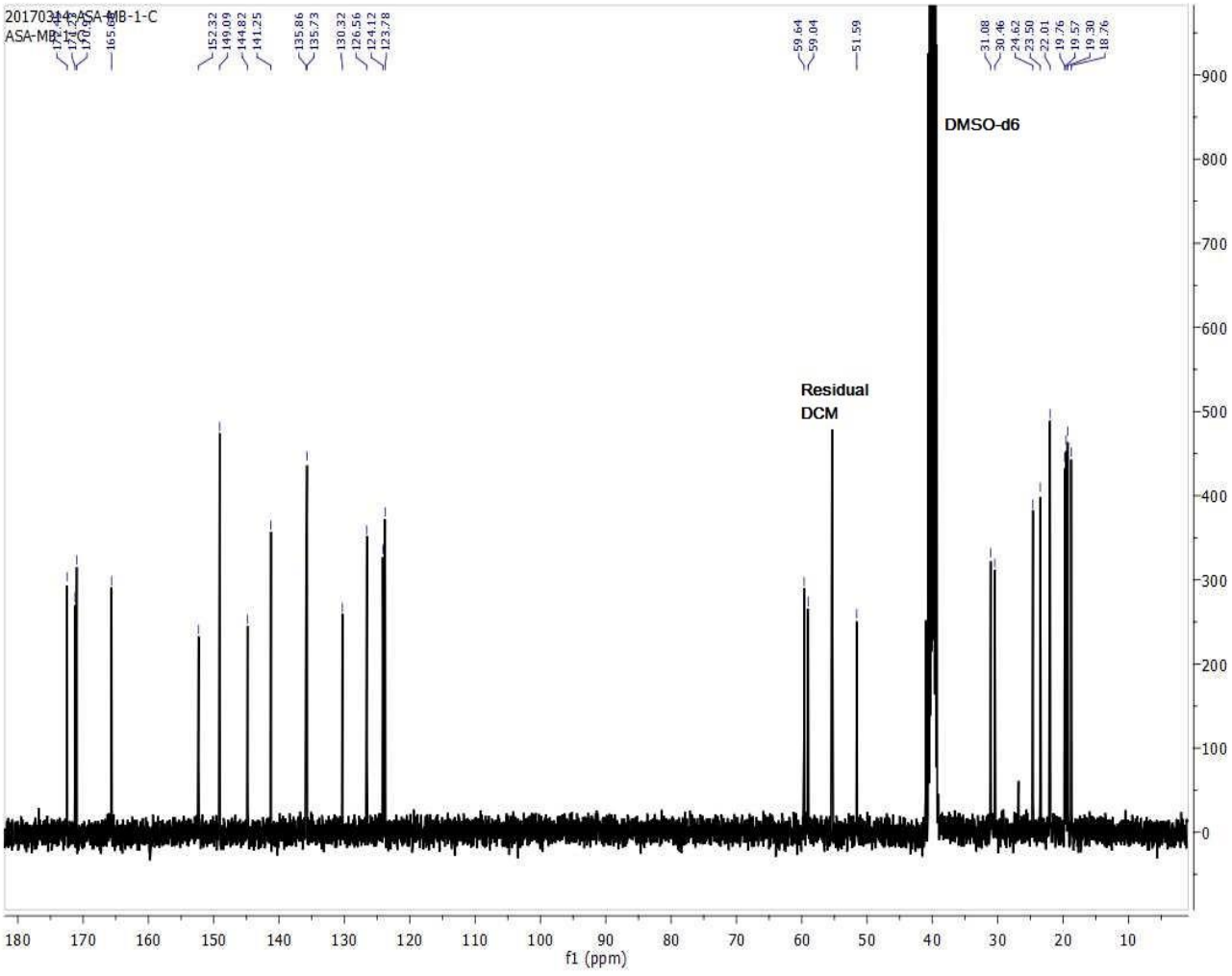

2.2.2) P2

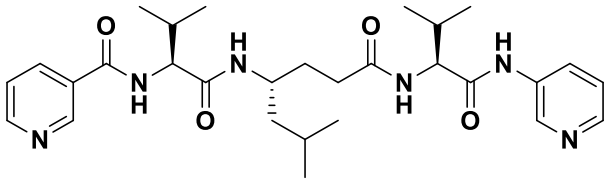

^{1}H NMR (400 MHz, DMSO-d$_6$) δ 10.22 (d, *J* = 10.7 Hz, 1H), 8.98 (dd, *J* = 6.5, 5.3 Hz, 1H), 8.76 – 8.70 (m, 1H), 8.66 (ddd, *J* = 4.7, 2.9, 1.7 Hz, 1H), 8.48 (dd, *J* = 13.7, 8.2 Hz, 1H), 8.21 (d, *J* = 4.6 Hz, 1H), 8.16 (dt, *J* = 8.0, 1.9 Hz, 1H), 8.05 – 7.95 (m, 2H), 7.89 – 7.71 (m, 1H), 7.50 – 7.41 (m, 1H), 7.33 – 7.24 (m, 1H), 4.24 – 4.14 (m, 2H), 3.77 (d, *J* = 4.3 Hz, 1H), 2.17 – 1.86 (m, 4H), 1.62 – 1.43 (m, 3H), 1.23 – 1.13 (m, 2H), 0.92 – 0.73 (m, 18H).

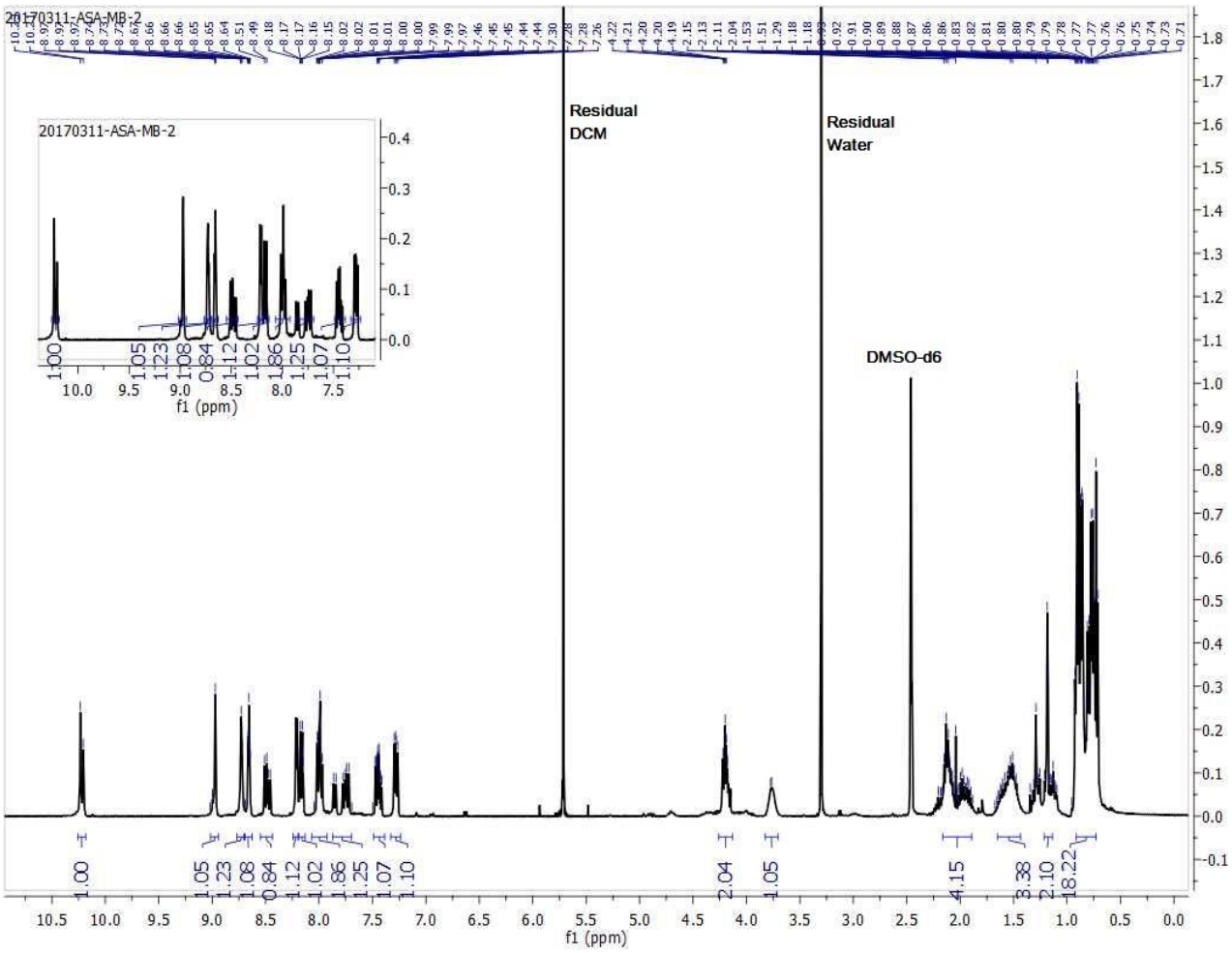

^{13}C NMR (101 MHz, DMSO-d$_6$) δ 173.01 (d, *J* = 15.5 Hz), 171.48 (s), 171.45 – 170.74 (m), 165.97 (s), 165.70 (s), 152.29 (s), 149.13 (d, *J* = 5.7 Hz), 144.74 (s), 141.45 (d, *J* = 6.1 Hz), 136.29 – 135.54 (m), 130.36 (d, *J* = 6.0 Hz), 126.70 (d, *J* = 5.0 Hz), 124.02 (s), 123.73 (d, *J* = 8.1 Hz), 60.11 (d, *J* = 8.7 Hz), 59.34 (s), 44.03 (d, *J* = 24.8 Hz), 43.86 – 43.54 (m), 32.32 (s), 31.80 (s), 30.73 (d, *J* = 13.9 Hz), 30.33 (d, *J* = 18.7 Hz), 29.45 (s), 24.80 (d, *J* = 16.2 Hz), 23.61 (d, *J* = 3.8 Hz), 22.16 (d, *J* = 10.6 Hz), 20.04 – 19.32 (m), 19.17 (s), 18.77 (d, *J* = 12.4 Hz).

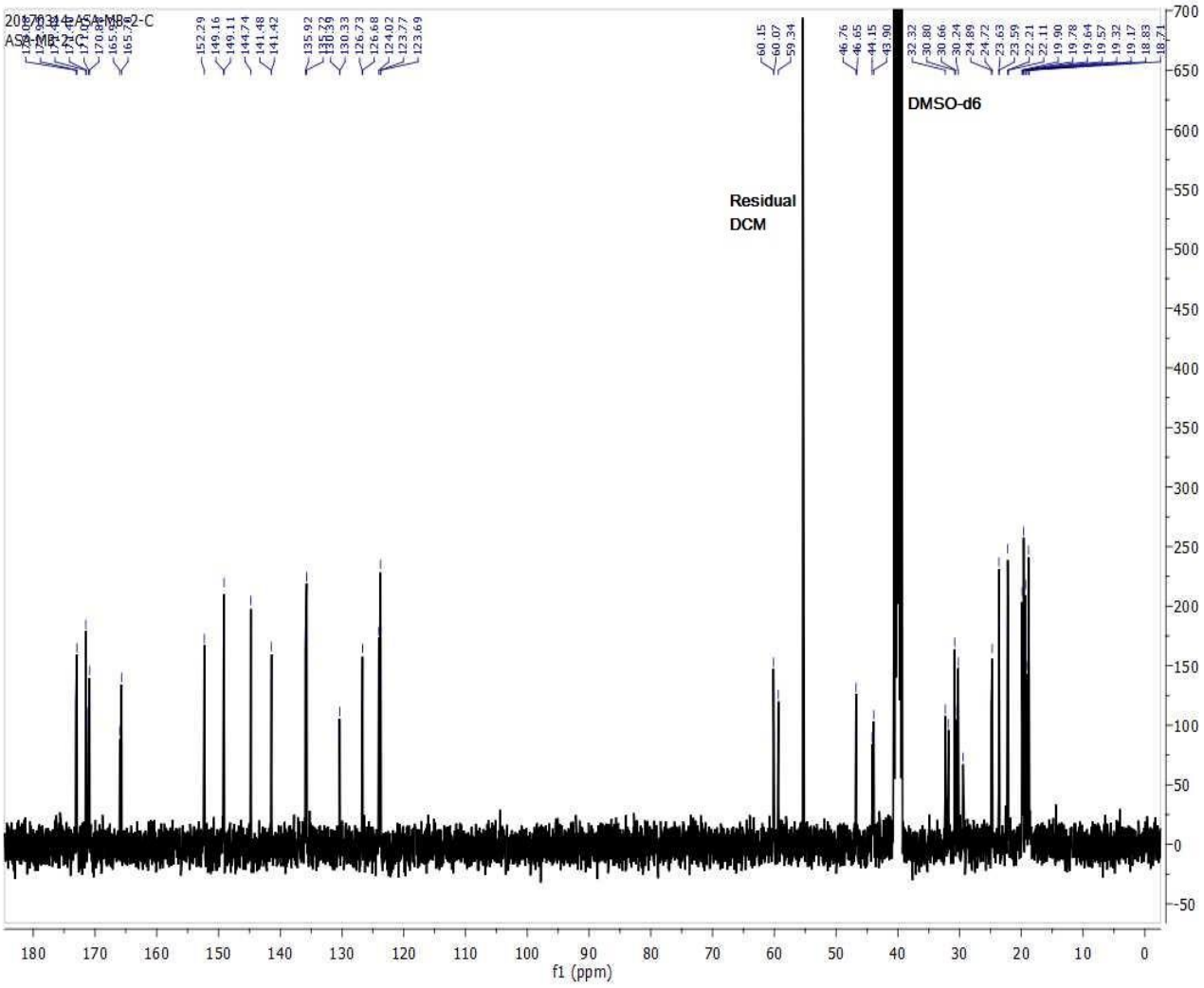

2.2.3) P3

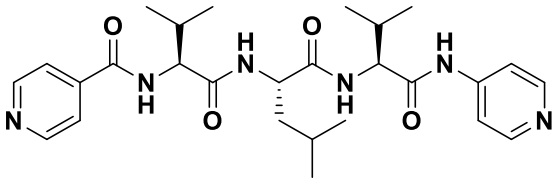

^{1}H NMR (400 MHz, DMSO-d$_6$) δ 10.48 – 10.32 (m, 1H), 8.70 – 8.57 (m, 3H), 8.41 – 8.31 (m, 2H), 8.18 – 8.08 (m, 1H), 7.97 (dd, *J* = 21.7, 8.1 Hz, 1H), 7.72 (dd, *J* = 8.8, 3.8 Hz, 2H), 7.50 (ddd, *J* = 13.0, 11.4, 5.6 Hz, 2H), 4.37 (dd, *J* = 14.5, 7.8 Hz, 1H), 4.26 (td, *J* = 15.1, 7.4 Hz, 2H), 2.10 – 1.93 (m, 2H), 1.63 – 1.52 (m, 1H), 1.50 – 1.36 (m, 2H), 0.89 – 0.74 (m, 17H).

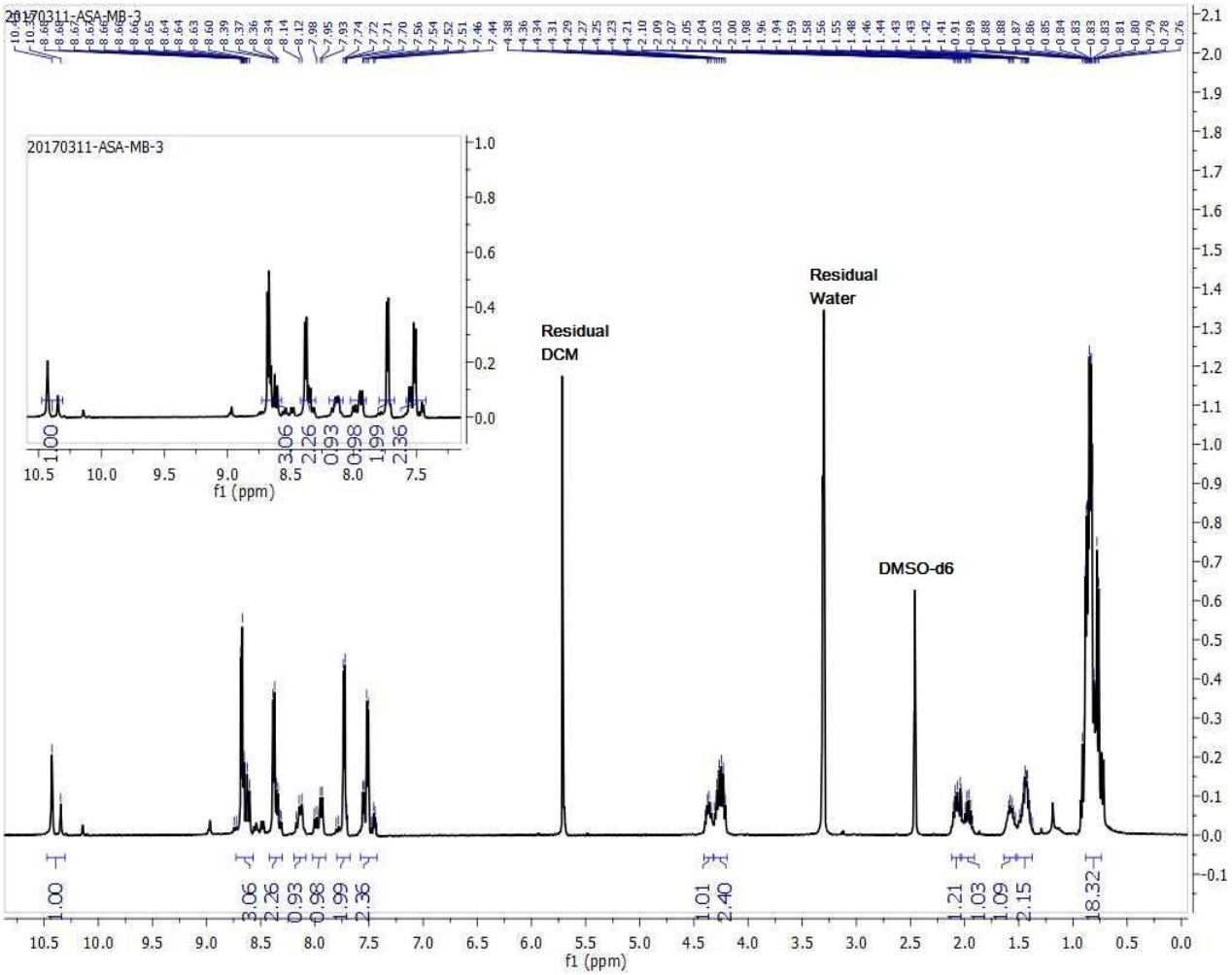

^{13}C NMR (101 MHz, DMSO-d$_6$) δ 172.73 (s), 172.51 (s), 171.72 (d, J = 6.1 Hz), 171.07 (s), 165.58 (d, J = 12.3 Hz), 150.86 (s), 150.49 (d, J = 14.3 Hz), 145.72 (s), 141.70 (s), 141.38 (s), 121.99 (s), 113.67 (s), 60.06 (s), 59.68 (s), 59.26 (s), 51.54 (s), 30.94 (s), 30.54 (d, J = 17.3 Hz), 24.62 (s), 23.49 (s), 22.02 (s), 21.62 (s), 19.51 (dd, J = 23.8, 18.2 Hz), 18.61 (d, J = 19.8 Hz).

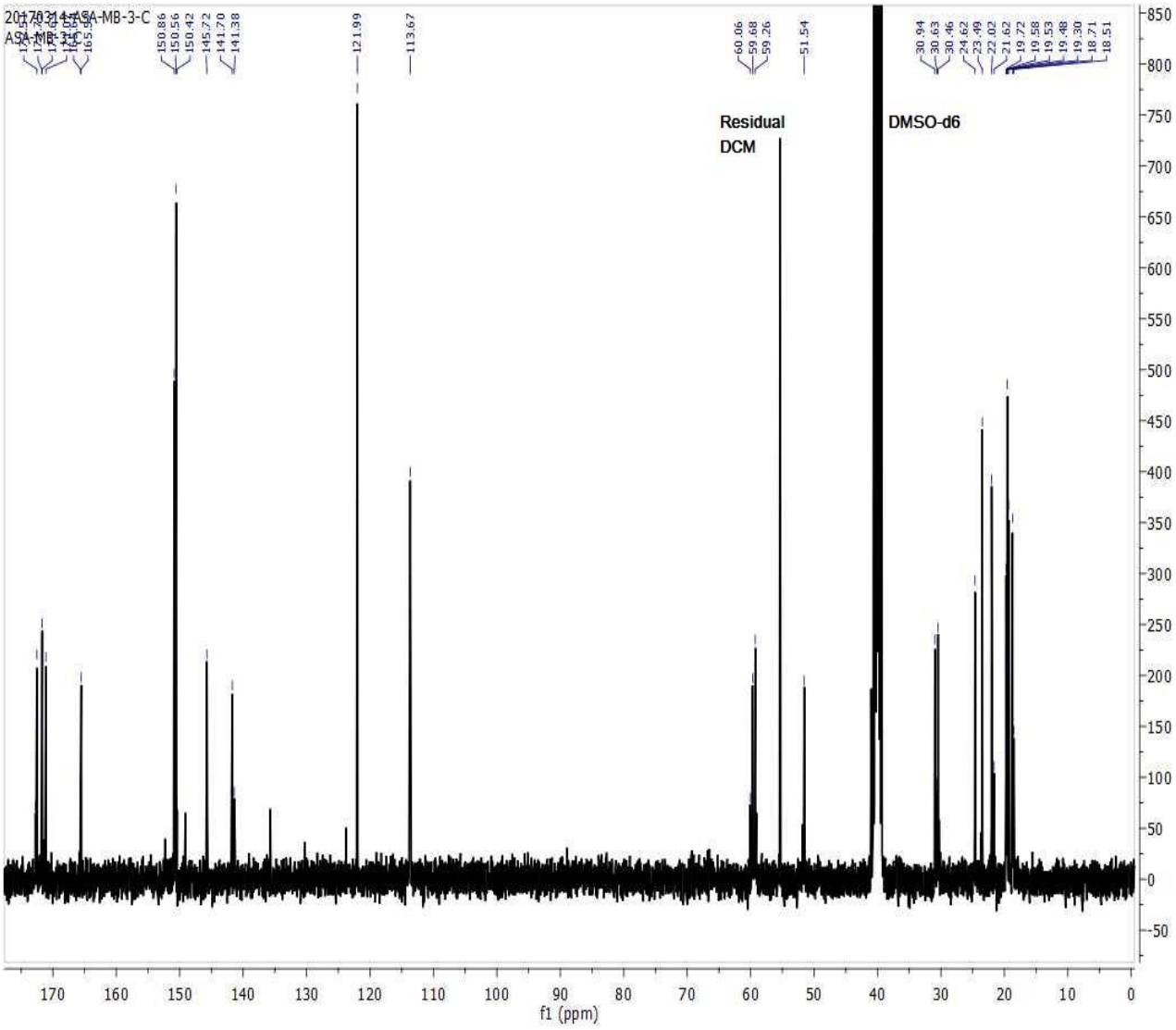

2.2.4) P4

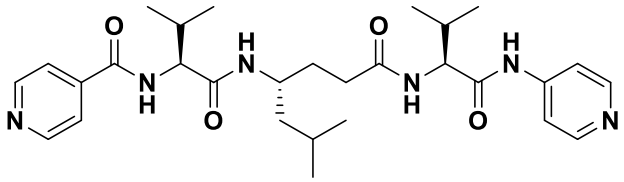

^{1}H NMR (400 MHz, DMSO-d$_6$) δ 10.46 – 10.36 (m, 1H), 8.67 (t, *J* = 5.1 Hz, 2H), 8.61 – 8.48 (m, 1H), 8.36 (t, *J* = 5.6 Hz, 2H), 8.05 – 7.88 (m, 1H), 7.84 – 7.68 (m, 3H), 7.58 – 7.50 (m, 2H), 4.21 (tt, *J* = 8.4, 6.8 Hz, 2H), 3.77 (s, 1H), 2.21 – 2.05 (m, 3H), 1.94 (qd, *J* = 13.5, 6.7 Hz, 1H), 1.63 – 1.45 (m, 3H), 1.29 (dt, *J* = 14.4, 6.0 Hz, 1H), 1.18 – 1.10 (m, 1H), 0.91 – 0.73 (m, 18H).

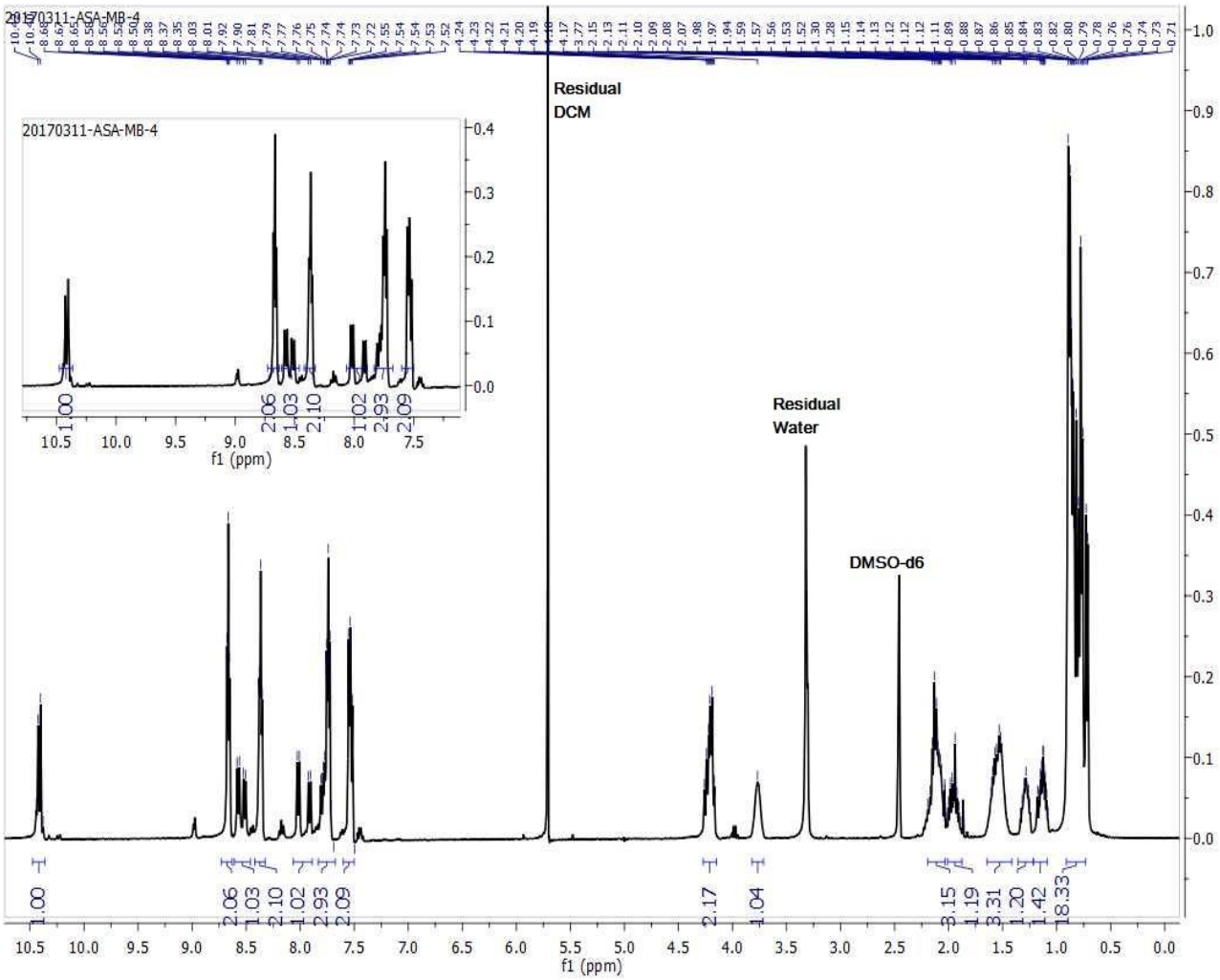

^{13}C NMR (101 MHz, DMSO-d$_6$) δ 172.96 (d, *J* = 5.4 Hz), 172.20 (d, *J* = 2.9 Hz), 170.73 (d, *J* = 5.0 Hz), 165.58 (d, *J* = 5.4 Hz), 150.80 (d, *J* = 4.2 Hz), 150.52 (d, *J* = 4.6 Hz), 145.80 (s), 141.78 (s), 122.03 (d, *J* = 6.5 Hz), 113.73 (d, *J* = 5.4 Hz), 60.11 (d, *J* = 19.2 Hz), 59.54 (s), 59.20 (s), 46.81 (s), 44.29 – 44.19 (m), 44.00 (d, *J* = 29.1 Hz), 32.46 (s), 32.19 (d, *J* = 20.9 Hz), 31.80 (s), 30.77 (d, *J* = 12.5 Hz), 30.44 (s), 30.21 (s), 24.78 (d, *J* = 12.6 Hz), 23.65 (d, *J* = 3.1 Hz), 22.17 (d, *J* = 8.1 Hz), 20.24 – 19.46 (m), 19.26 (d, *J* = 12.4 Hz), 18.76 (d, *J* = 9.7 Hz).

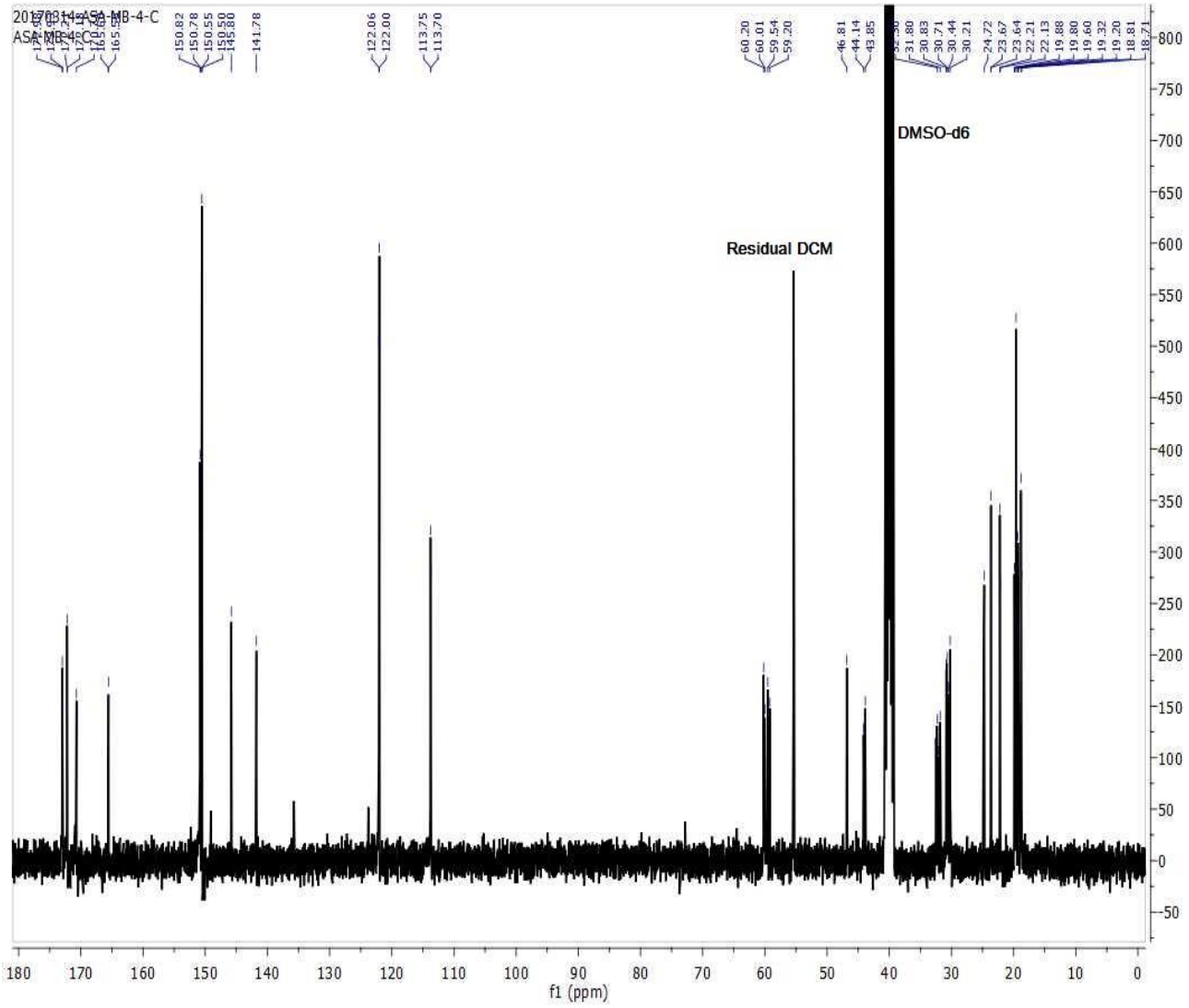

2.2.5) P5

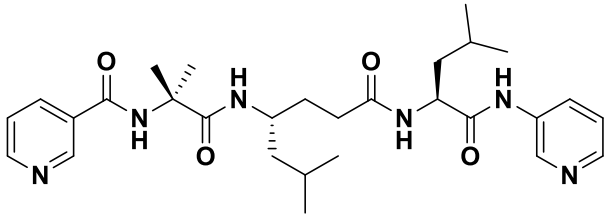

^{1}H NMR (400 MHz, DMSO-d$_6$) *δ* 10.18 (s, 1H), 9.01 (dd, *J* = 2.2, 0.7 Hz, 1H), 8.78 (d, *J* = 2.4 Hz, 1H), 8.69 – 8.65 (m, 1H), 8.60 (s, 1H), 8.20 (dd, *J* = 4.7, 1.5 Hz, 1H), 8.19 – 8.15 (m, 1H), 8.05 (ddd, *J* = 8.4, 2.5, 1.5 Hz, 1H), 7.82 (d, *J* = 6.9 Hz, 1H), 7.51 (d, *J* = 9.3 Hz, 1H), 7.46 (ddd, *J* = 7.9, 4.8, 0.8 Hz, 1H), 7.31 – 7.23 (m, 1H), 4.20 (dt, *J* = 9.0, 6.4 Hz, 1H), 3.75 (qd, *J* = 9.5, 5.1 Hz, 1H), 2.21 – 2.12 (m, 1H), 2.05 (ddd, *J* = 8.4, 6.7, 5.0 Hz, 1H), 1.70 – 1.60 (m, 2H), 1.47 (d, *J* = 9.1 Hz, 6H), 1.45 – 1.36 (m, 4H), 1.34 – 1.25 (m, 1H), 1.08 (ddd, *J* = 13.5, 8.8, 4.7 Hz, 1H), 0.83 – 0.76 (m, 6H), 0.69 (dd, *J* = 6.6, 3.8 Hz, 6H).

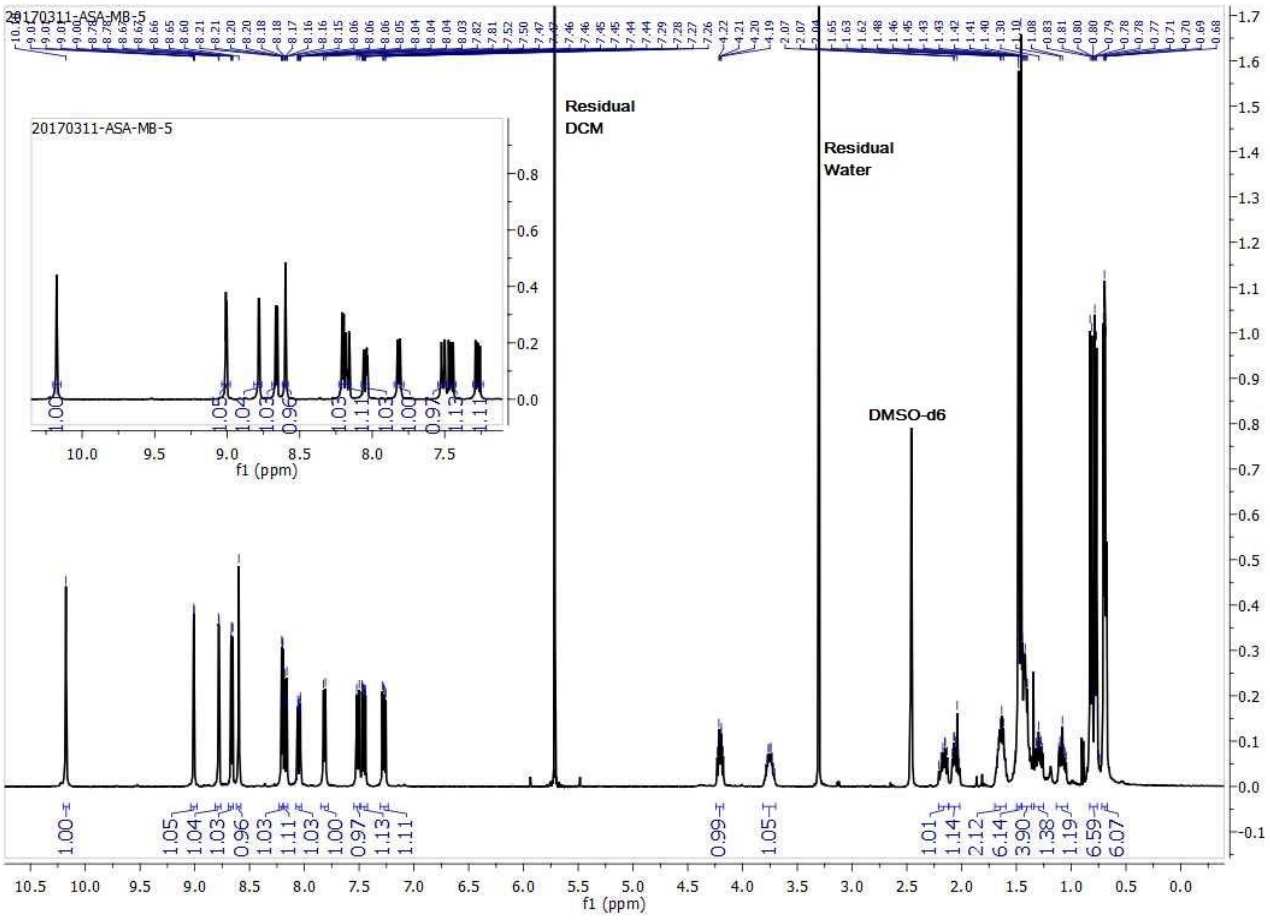

^{13}C NMR (101 MHz, DMSO-d$_6$) δ 174.37 (s), 173.19 (s), 172.51 (s), 165.51 (s), 152.31 (s), 149.19 (s), 144.70 (s), 141.73 (s), 136.10 (s), 135.70 (s), 130.59 (s), 126.95 (s), 123.79 (d, *J* = 15.2 Hz), 57.22 (s), 53.36 (s), 46.34 (s), 44.54 (s), 32.12 (s), 31.84 (s), 25.90 (s), 25.45 (s), 24.77 (d, *J* = 1.7 Hz), 23.50 (s), 23.26 (s), 22.36 (s), 21.92 (s).

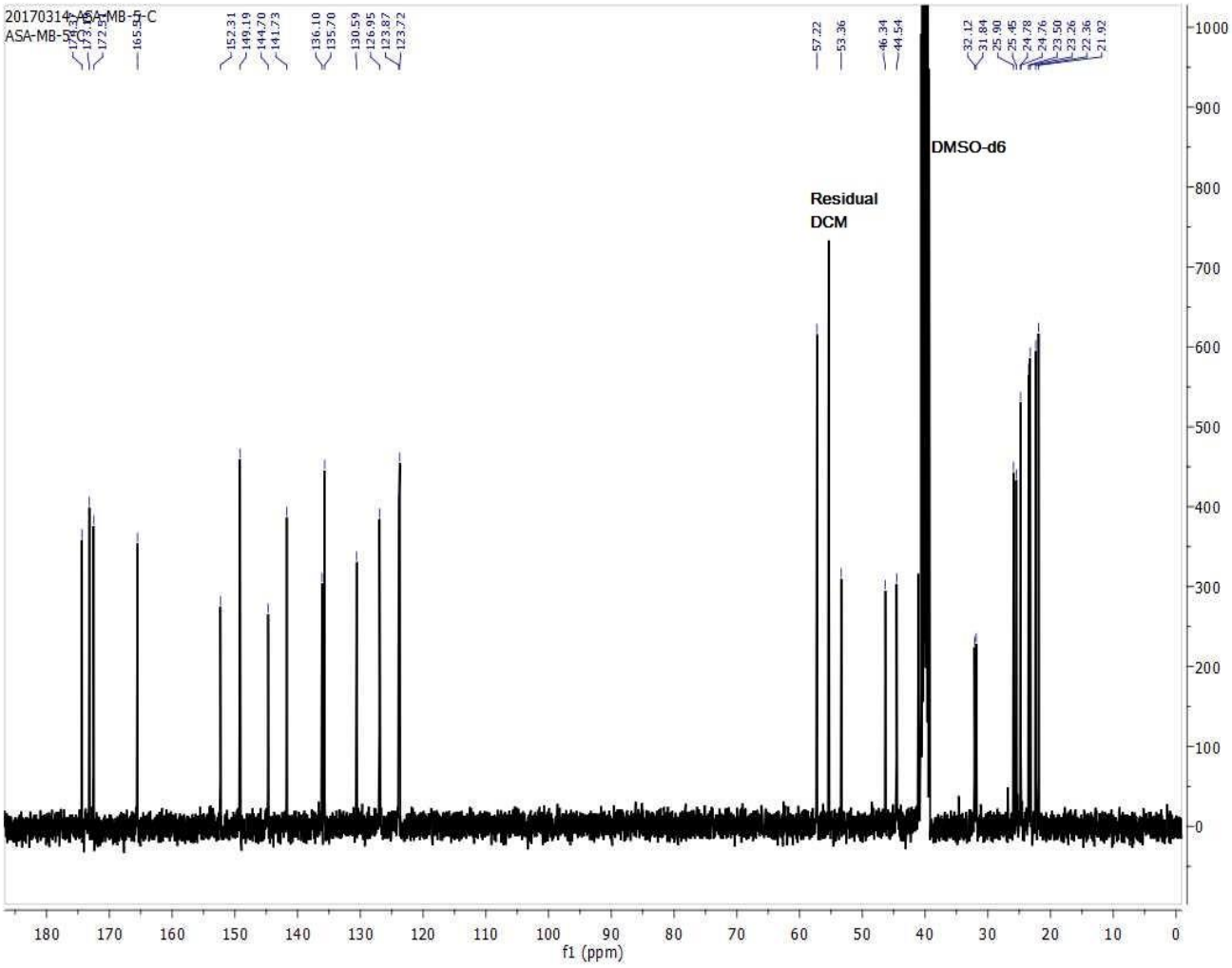

3) RESULTS AND DISCUSSIONS

3.1) Structural Studies of Peptides

As single crystals provide unambiguous structural information, we subjected all of the peptides to crystallization in various solvent combinations. However, due to the high aggregating nature of β-sheets, peptides **P1** and **P3** resulted in the formation of fibrous aggregates. Nevertheless, **P2** and **P4** gave X-ray quality single crystals methanol/chloroform solvent combinations. Crystals of **P5** were grown from a

concentrated solution of peptide in aqueous methanol. Detailed conformational analysis of the peptides is given below. The X-ray structures along with H-bonding patterns are shown in Figure 2. Surprisingly, all three tripeptides **P2**, **P4** and **P5** adopted well folded 12-helical conformations in single crystals. The 12-helices are stabilized by the two intramolecular H-bonds between the residues *i* and *i+3*. The backbone torsion angles of the γ-resides can be measured by introducing two additional variables θ_1 and θ_2 along with ϕ and ψ. The local torsion variables of γ-residues are shown in Figure 3. Backbone torsional angles and hydrogen bonding parameters of these α/γ4-hybrid peptides are listed in Table 1 and Table 2, respectively.

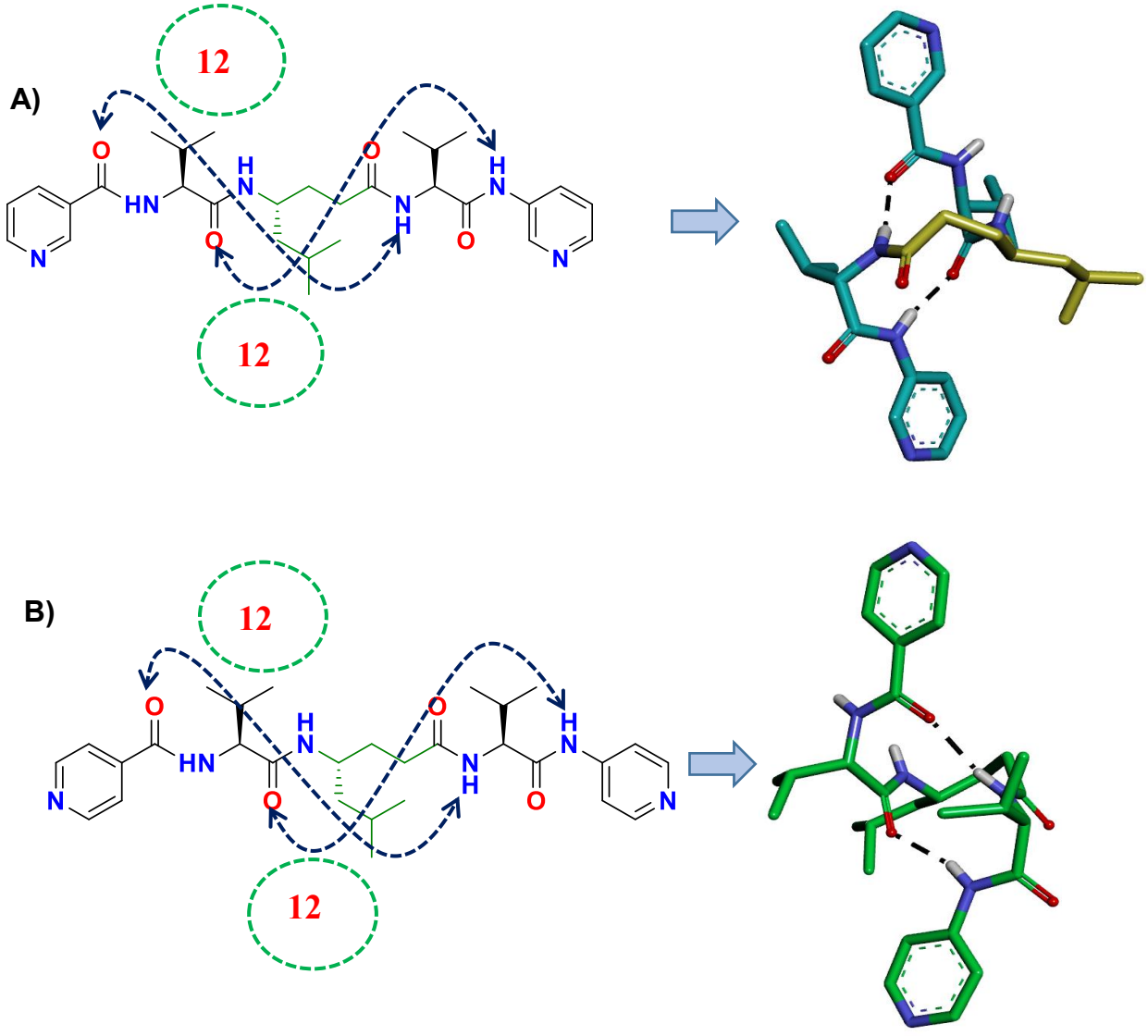

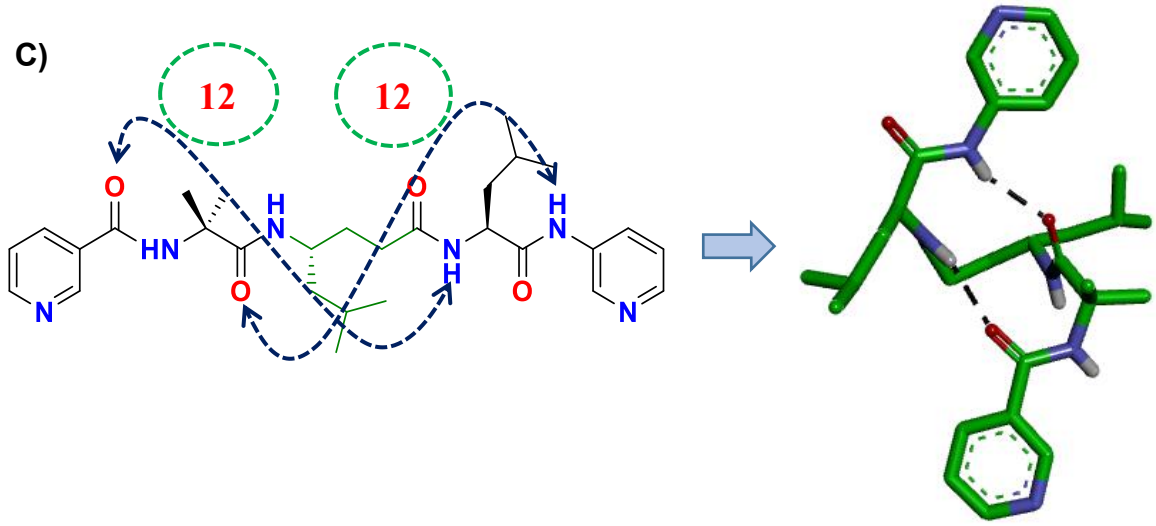

Figure 2: Hydrogen bonding schemes and crystal structures of A) P2, B) P4 and C) P5

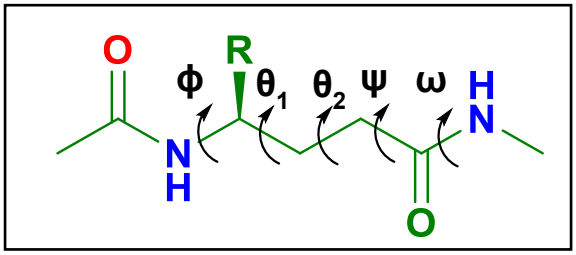

Figure 3: Torsional variables in γ-peptides.

Peptide	Residue	ϕ	θ1	θ2	ψ	ω
		In degrees				
P2	Val 1	-69	-	-	-40	-176
	γ^4 Leu 2	-122	44	69	-119	-173
	Val 3	-64	-	-	-38	-170
P4	Val 1	-81	-	-	-26	-180
	γ^4 Leu 2	-117	45	63	-131	-171
	Val 3	-62	-	-	-41	-172
P5	Aib 1	-57	-	-	-44	-170
	γ^4 Leu 2	-122	48	69	-117	-168
	Leu 3	-88	-	-	-20	-178

Table 1: Backbone torsional angles of α/γ4-hybrid peptides P2, P4 and P5.

Peptide	Hydrogen Bond	C=O ----- H	C=O ----- N	∟O-----H-N
		in angstroms		In degrees
P2	Py CO⟶Val (3) NH	2.08	2.93	167
	Val (1) CO⟶ NH Py	2.09	2.92	161
P4	Py CO⟶Val (3) NH	2.04	2.89	169
	Val (1) CO⟶ NH Py	2.12	2.94	161
P5	Py CO⟶Leu (3) NH	2.23	3.06	161
	Aib (1) CO⟶ NH Py	2.12	2.93	157

Table 2: Hydrogen bonding parameters of α/γ4-hybrid peptides P2, P4 and P5.

3.2) Metalation Studies of Peptides

All peptides were further subjected to metalation studies to understand their metal driven self-assembly behaviour. Ag^+ was chosen as the model metal ion for the peptides with 3-pyridyl groups and Cu^{2+} as the model metal ion for the peptides with 4-pyridyl groups.

3.2.1) Ag^+ Driven Self-assembly of P1

In order to understand the behavior of the beta sheet peptide **P1** with metals, it was subjected to the metalation studies with Ag^+. The methanolic solution of **P1** (500 µL of 25 mM of **P1** in MeOH) was added to 500 µL of 25 mM of an ethanolic solution of $AgBF_4$ in a glass vial. The resulting mixture was sonicated for 1 minute. Instantaneously, the formation of a stable gel was observed, which was confirmed by the vial inversion method. The ratio between the metal and the peptide was varied to understand the role of stoichiometry in the gelation. Metalation studies were carried out using different equivalents (0, 0.25, 0.50, 0.75 and 1) of $AgBF_4$. The most robust gelation was found when the peptide was treated with one equivalent of $AgBF_4$. Peptide alone did not lead to the gelation. On using less than one equivalent of $AgBF_4$ produced weak and unstable gels. Increasing the concentration of $AgBF_4$ beyond one equivalent did not make any

considerable differences. Thereby, these results indicate the possibility of 1:1 complexation between the peptide and metal. The minimum gelator concentration was found to be 8 mM. Although **P1** was further screened for the metalation studies with Cu^{2+}, Zn^{2+}, Co^{2+} and Ni^{2+}, immediate precipitation of the complexes was observed in all the cases. Nanoscale morphology analysis of the metallogel was carried out using FE-SEM, which revealed the presence of entangled fibrous networks, as expected.

Due to the inherent aggregating nature of β-sheet peptides through strong intermolecular hydrogen bonding, the formation of the supramolecular gel upon metal coordination is not surprising. The coordination polymers formed upon metal coordination can undergo aggregation through these strong secondary interactions between the peptide backbones, resulting in the formation of stable supramolecular metallogels.

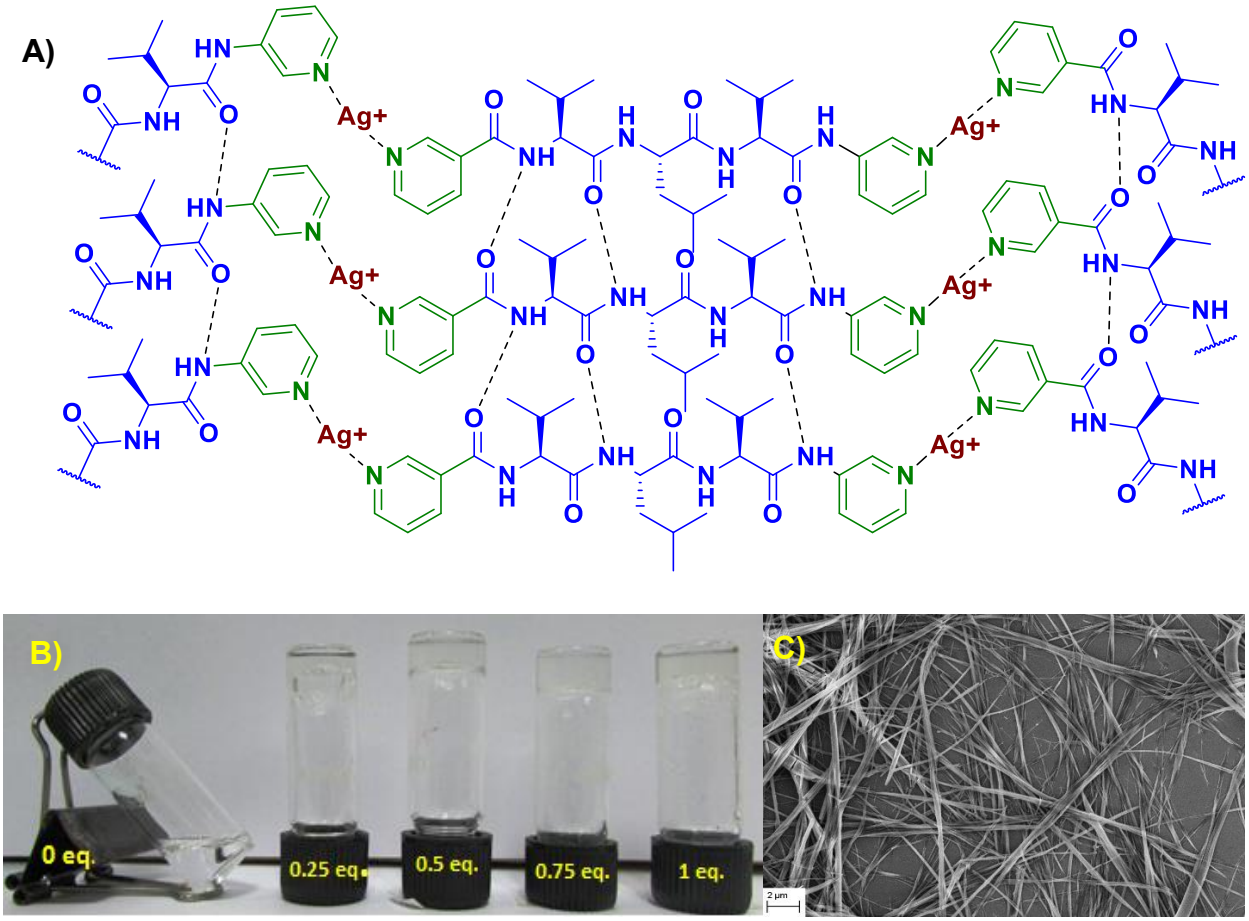

Figure 4: A) Proposed binding of Ag^{+} and P1, B) Images of the metallogels prepared by varying the equivalents of $AgBF_4$, C) FE-SEM image of the metallogel prepared using 1 equivalent of $AgBF_4$.

3.2.2) Ag^+ Driven Self-assembly of P2

In order to understand the behavior of the helical peptide **P2** with metals, it was subjected to the metalation studies with Ag^+. The solution of peptide **P2** in chloroform (500 µL of 25 mM) and 500 µL of 25 mM of an ethanolic solution of $AgBF_4$ were mixed in a glass vial. The resulting mixture was sonicated for 1 minute. Interestingly, the formation of a stable gel was observed after 6 hours. The ratio between the metal and the peptide was varied to understand the role of stoichiometry in gelation. As in the case of **P1**, the most robust gelation was found when the peptide was treated with one equivalent of $AgBF_4$, indicating 1:1 complexation. The minimum gelator concentration was found to be 12 mM. Morphology investigations carried out through FE-SEM revealed the presence of entangled nanofibrous networks.

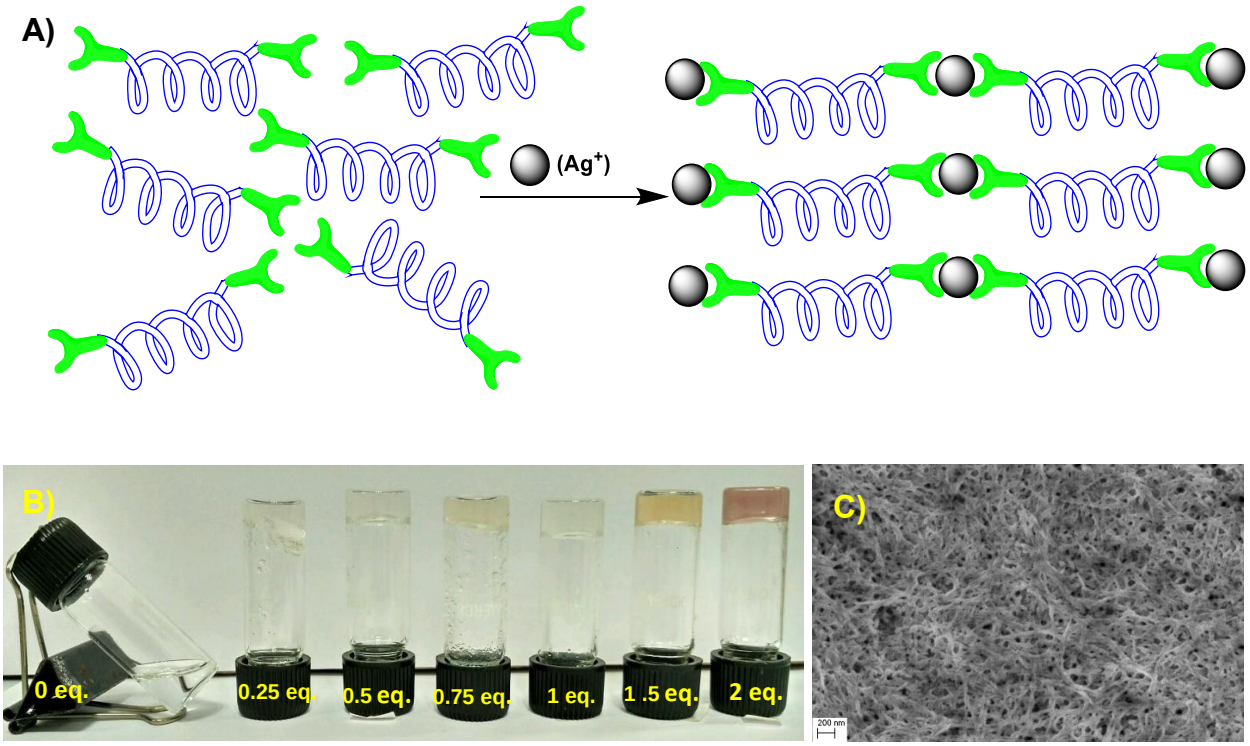

Figure 5: A) A cartoon representation on Ag^+ driven self-assembly of P2, B) Images of the metallogels prepared using different equivalents of $AgBF_4$, C) FE-SEM image of the metallogel prepared using 1 equivalent of $AgBF_4$.

So far, there are hardly any reports on the metal driven gelation of helical peptide foldamer ligands. Compared to β -sheet peptides, which already have an inherent aggregating property through strong intermolecular hydrogen bonding, the intermolecular interactions between helical peptides are very limited, as evident from the crystal structure. So, the driving force for the formation of metallogel from the helical peptide ligand is yet to be understood. Detailed investigative studies on the mechanism of gelation are currently in progress.

3.2.3) Cu^{2+} Driven Self-assembly of P3

To understand the behavior of the β-sheet peptide **P3** with metals, it was subjected to the metalation studies with Cu^{2+}. The peptide solution in chloroform (500 µL of 30 mM) and 500 µL of 30 mM of an ethanolic solution of $CuCl_2.3H_2O$ was mixed in a glass vial. The resulting mixture was sonicated for 1 minute. Formation of a stable gel was observed after one hour, which was confirmed by the vial inversion method. Different equivalents of $CuCl_2.3H_2O$ (0, 0.25, 0.50, 0.75, 1, 1.50 and 2) were used for the gelation studies to understand the role of stoichiometry in gelation. Interestingly, immediate gelation was observed when the peptide to metal ratio was either 1:1 or 2:1. This clearly indicates that there can be two possibilities of coordination.

We hypothesize that in the first case, where peptide to metal ratio is 1:1, each Cu^{2+} can form a tetrahedral complex in which two pyridyl ligands from the peptides and two chlorine ligands can coordinate to a single metal center. The resulting coordination polymer can aggregate through the secondary interactions from the β-sheet peptide backbone, leading to the formation of stable metallogels.

In the second case, where the peptide to metal ratio is 2:1, the tetrahedral complex formed by each metal center might be exclusively coordinated by the pyridyl ligands from the peptides. Again, the resulting coordination polymer can undergo aggregation through the secondary interactions from the β-sheet peptide backbone, leading to the formation of nanofibers and thereby constructing stable metallogels. The two modes of binding are shown in Figure 5.

The minimum gelator concentration was found to be 15 mM. **P3** was also found to gelate with Ag^{+} in an equimolar ratio with a minimum gelator concentration of 10 mM. Although **P3** was further screened for the metalation studies with Zn^{2+}, Co^{2+} and Ni^{2+}, immediate precipitation of the complexes was observed in all the cases.

A)

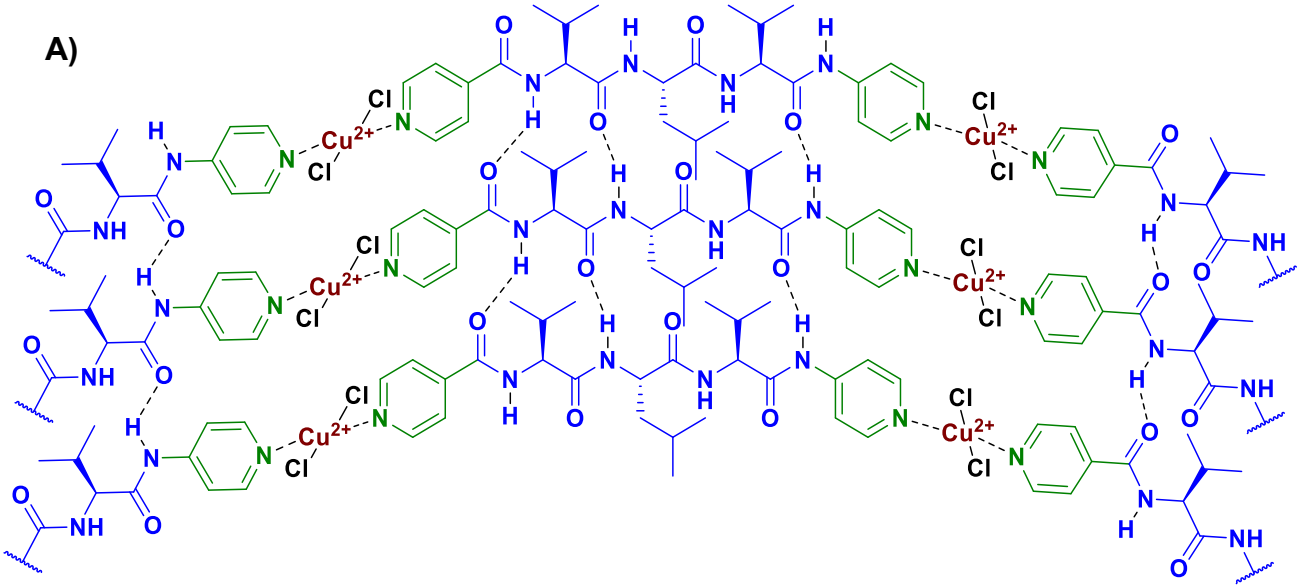

B)

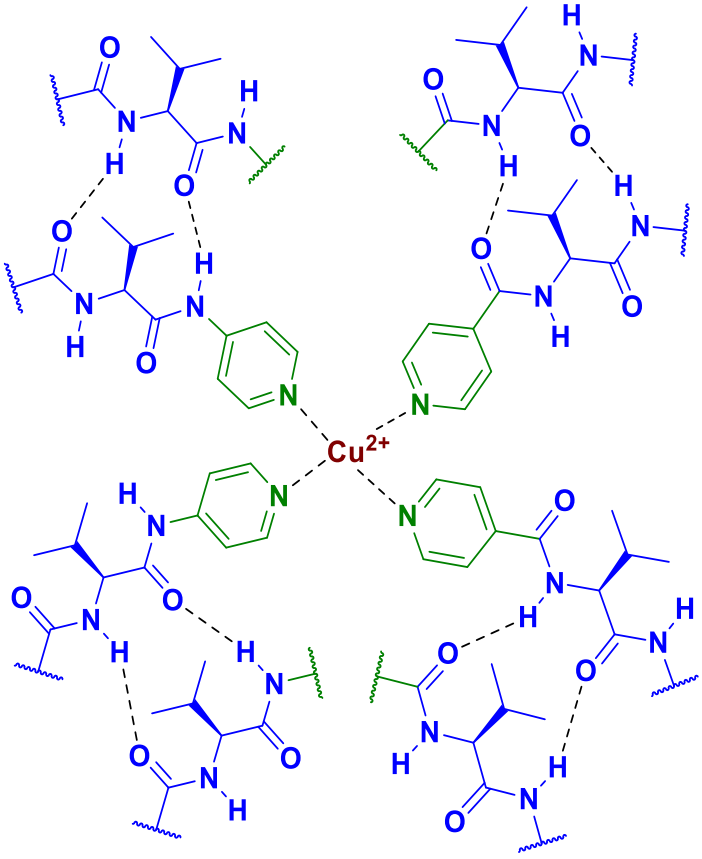

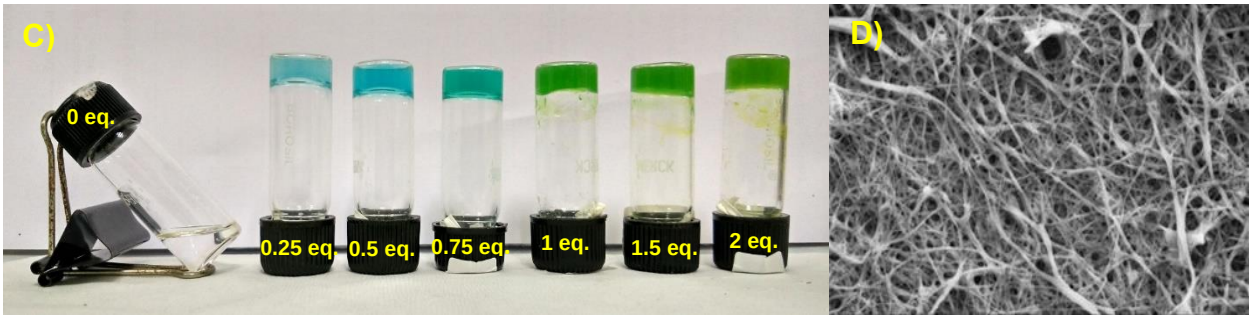

Figure 6: A) Proposed binding between Cu^{2+} and P3 in 1:1 ratio, B) Proposed binding between Cu^{2+} and P3 in 1:2 ratio, C) Images of the metallogels prepared by varying the equivalents of $CuCl_2.3H_2O$, D) FE-SEM image of the metallogel prepared using 1 equivalent of $CuCl_2.3H_2O$.

3.2.4) Cu^{2+} Driven Self-assembly of P4

In order to understand the behavior of helical peptide **P4** with metals, it was subjected to the metalation studies with Cu^{2+}. The solution of peptide in (500 µL of 30 mM) chloroform and 500 µL of 30 mM of an ethanolic solution of $CuCl_2.3H_2O$ were mixed in a glass vial. The resulting mixture was sonicated for 1 minute. Interestingly, the formation of a stable gel was observed after one hour and the gelation was confirmed by the vial inversion method. Different equivalents of $CuCl_2.3H_2O$ (0.50, 1, 1.50 and 2) were used for the gelation studies to understand the role of stoichiometry in gelation. As in the case of **P3**, stable gels were obtained for both 1:1 and 2:1 metal to peptide ratios, again indicating two possibilities of coordination between the peptide and metal. As stated before for **P3**, the tetrahedral complexes of Cu^{2+} can form either through the coordination of two pyridyl ligands from the peptide and two chlorine ligands (leading to 1:1 complexation of peptide and metal) or through the complete coordination of pyridyl ligands (leading to 2:1 complexation of peptide and metal). A representative cartoon diagram on the modes of binding is given in Figure 7. As in the case of **P2**, the mechanism of gelation of the helical peptide **P4** is unknown and the detailed experimental investigations are currently under progress. The minimum gelator concentration for **P4** was found to be 15 mM.

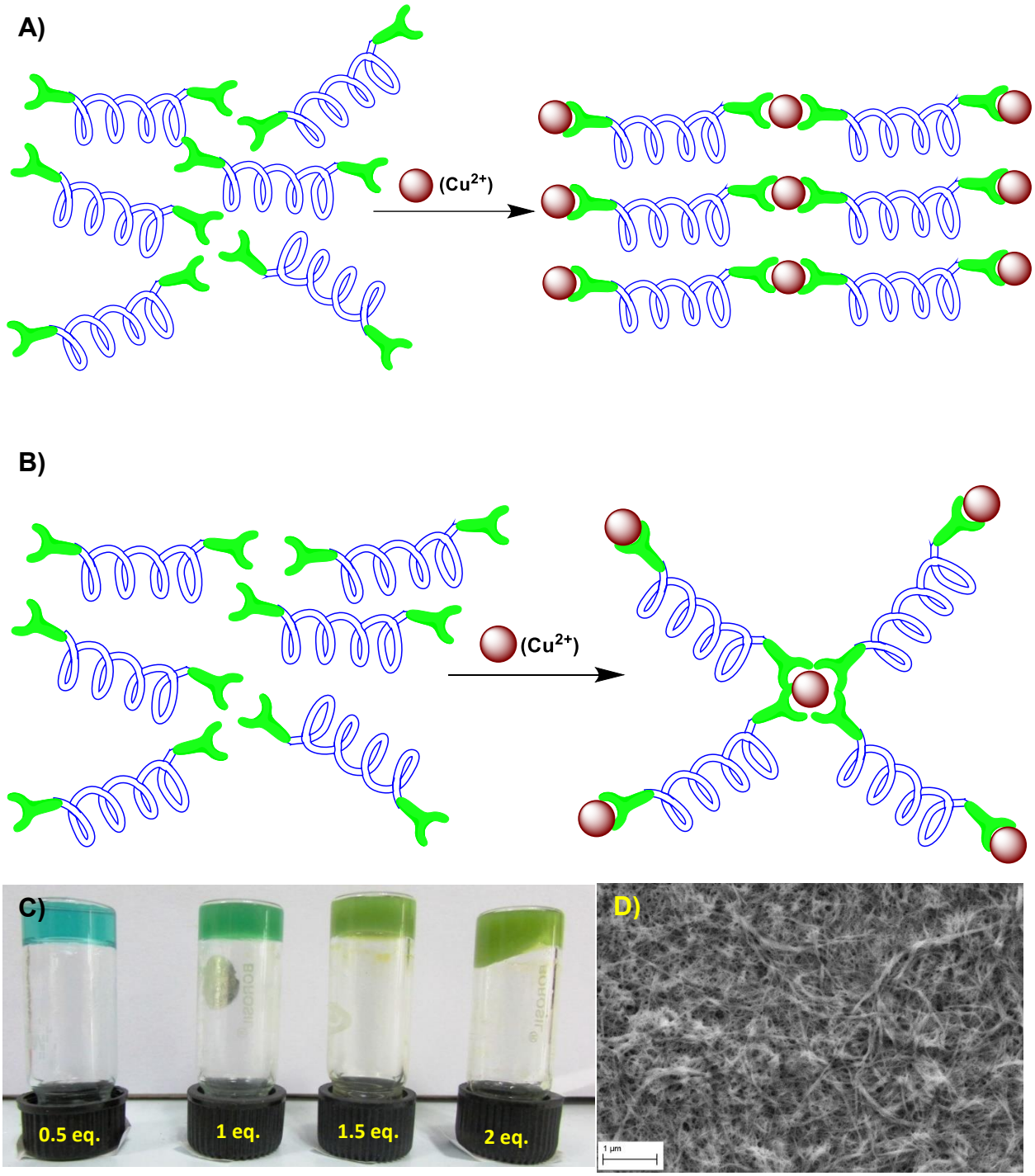

Figure 7: A) Proposed binding between Cu^{2+} and P3 in 1:1 ratio, B) Proposed binding between Cu^{2+} and P3 in 1:2 ratio, C) Images of the metallogels prepared by varying the equivalents of $CuCl_2.3H_2O$, C) FE-SEM image of the metallogel prepared using 1 equivalent of $CuCl_2.3H_2O$.

3.2.5) Ag^+ Driven Self-assembly of P5

The control helical peptide P5 was also subjected to metalation studies using Ag^+. The peptide solution in (500 µL of 25 mM) chloroform and 500 µL of 25 mM of an ethanolic solution of $AgBF_4$ were mixed in a glass vial followed by sonication. In contrast to **P2, P5** did not yield gels. However, we noticed the immediate formation of colorless block crystals within 15 to 20 min after mixing with the silver ions. Structural studies of the crystals obtained from MeOH/H_2O combination revealed that the peptide retains its helical structure in the complex. Apart from the 12-membered hydrogen bonding, the peptide within the complex is stabilized by a 9-membered hydrogen bonding as well. The detailed structural investigation of this complex is currently under progress. X-ray structure of the complex is given in figure 8.

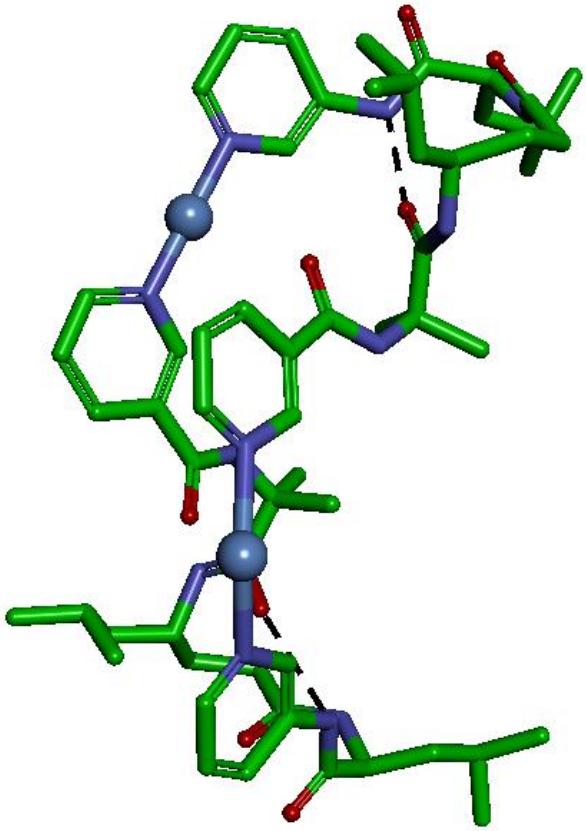

Figure 8: X-ray structure of the Complex of P5 and Ag(I)

In a sharp contrast to the helical peptides **P2** and **P4**, where the supramolecular assembly driven by metal coordination led to the formation of metallogels, the unique behavior of **P5** is quite interesting. The reason for this different behavior is not yet understood. We speculate that, in the cases of **P2** and **P4**, there is a possibility of structural transformation from helix to β-sheet upon metal binding, which may not be possible in the case **P5**. Moreover, the β-branched amino acid valine, being an inherent sheet promoter motif, might make the helices **P2** and **P4** a bit unstable compared to **P5**. On the basis of these observations, we hypothesize that the metal coordination driven gelation from **P2** and **P4** can possibly arise from the coordination driven unfolding of these helical foldamers. The unfolded peptide might offer the required secondary interactions for the further aggregations, leading to gelation. However, we are further investigating to find the reason for this special behavior of **P5**. Detailed investigations on the mechanism of gelation from the helical foldamers P2 and P4 are currently under progress.

4) CONCLUSIONS

In conclusion, we have successfully shown the formation of stable metallogels through coordination driven assembly of peptide ligands. Stable metallogels of Ag(I) and Cu(II) could be constructed from a β-sheet peptide template Val-Leu-Val. Structural transformation from β-sheet to C-12 helix could be observed upon replacing leucine with γ-leucine in these sequences. The resulted helical foldamers were well characterized by X-ray analysis. Quite surprisingly, the helical foldamers were also found to form metallogels through metal mediated self-assembly. To the best of our knowledge, this is the first report on the metallogels arising from helical peptide foldamers. The contrasting results obtained from the control helical peptide indicates the possibility of metal coordination driven unfolding of the helical foldamers. We are currently studying the mechanism of gelation from the helical foldamers. The evaluation of the catalytic properties of these metallogels is also in progress. Overall, results reported in this work can be further explored to design functional foldamer metallogels.

References

1) Permyakov, E. A. Metalloproteomics, *John Wiley & Sons, Inc.*, **2009**, 7–19.

2) Albrecht, M.; Stortz, P. Metallacyclopeptides: Artificial analogues of naturally occurring peptides. *Chem. Soc. Rev.*, **2005**, *34*, 496–506.

3) Alies, B.; Hureau, C.; Faller, P. The role of metal ions in amyloid formation: general principles from model peptides. *Metallomics*, **2013**, *5*, 183–192.

4) Zhang, S. Fabrication of novel biomaterials through molecular self-assembly. *Nat. Biotechnol.*, **2003**, *21*, 1171–1178.

5) Li, H.; Eddaoudi, M.; O'Keeffe, M.; Yaghi, O. M. Design and synthesis of an exceptionally stable and highly porous metal-organic framework. *Nature*, **1999**, *402*, 276-279.

6) Zhukhovitskiy, A. V.; Zhong, M.; Keeler, E. G.; Michaelis, V. K.; Sun, J. E. P.; Hore, M. J. A.; Pochan, D. J.; Griffin, R. G.; Willard, A. P.; Johnson, J. A. Highly branched and loop-rich gels via formation of metal–organic cages linked by polymers *Nat. Chem.*, **2016**, *8*, 33-41.

7) Riddell, I. A.; Smulders, M. M. J.; Clegg, J. K.; Hristova, Y. R.; Breiner, B.; Thoburn, J. D.; Nitschke, J. R. Anion-induced reconstitution of a self-assembling system to express a chloride-binding $Co_{10}L_{15}$ pentagonal prism. *Nat. Chem.*, **2012**, *4*, 751-756.

8) Yoshizawa, M.; Tamura, M.; Fujita, M. Diels-alder in aqueous molecular hosts: unusual regioselectivity and efficient catalysis. *Science*, **2006**, *312*, 251–254.

9) Wang, J.; He, C.; Wu, P.; Wang, J.; Duan, C. An Amide-Containing Metal–Organic Tetrahedron Responding to a Spin-Trapping Reaction in a Fluorescent Enhancement Manner for Biological Imaging of NO in Living Cells. *J. Am. Chem.Soc.*, **2011**, *133*, 12402-12405.

10) Whitesides, G. M.; Mathias, J. P.; Set, C. T. Molecular self-assembly and nanochemistry: a chemical strategy for the synthesis of nanostructures, *Science*, **1991**, *254*, 1312-1319.

11) Stupp, S. I.; Palmer, L. C. Supramolecular Chemistry and Self-Assembly in Organic Materials Design, *Chem. Mater.*, **2014**, *26*, 507-518.

12) Lakshmanan, A.; Zhang, S.; Hauser, C. A. E. Short self-assembling peptides as building blocks for modern nanodevices. *Trends Biotechnol.* **2012**, *30*, 155-165.

13) Zelzer, M.; Ulijn, R. V. Next-generation peptide nanomaterials: molecular networks, interfaces and supramolecular functionality. *Chem. Soc. Rev.*, **2010**, *39*, 3351-3357.

14) Gazit, E. Self-assembled peptide nanostructures: the design of molecular building blocks and their technological utilization. *Chem. Soc. Rev.*, **2007**, *36*, 1263-1269.

15) Hamley, I. W. Self-assembly of amphiphilic peptides. *Soft Matter*, **2011**, *7*, 4122-4138.

16) Przybyla, D. E.; Rubert Pe´rez, C. M.; Gleaton, J.; Nandwana, V.; Chmielewski, J. Hierarchical Assembly of Collagen Peptide Triple Helices into Curved Disks and Metal Ion-Promoted Hollow Spheres. *J. Am. Chem. Soc.*, **2013**, *135*, 3418–3422.

17) Nepal, M.; Sheedlo, M. J.; Das, C.; Chmielewski, J. Accessing Three-Dimensional Crystals with Incorporated Guests through Metal-Directed Coiled-Coil Peptide Assembly. *J. Am. Chem. Soc.*, **2016**, *138*, 11051-11057.

18) Tavenor, N. A.; Murnin, M. J.; Horne, W. S. Supramolecular Metal-Coordination Polymers, Nets, and Frameworks from Synthetic Coiled-Coil Peptides. *J. Am. Chem. Soc.*, **2017**, *139 (6)*, 2212–2215.

19) Sawada, T.; Matsumoto, A.; Fujita, M. Coordination-driven folding and assembly of a short peptide into a protein-like two-nanometer-sized channel. *Angew. Chem. Int. Ed.*, **2014**, *53*, 7228-7232.

20) Sawada, T.; Yamagami, M.; Ohara, K.; Yamaguchi, K.; Fujita, M. Peptide [4]Catenane by Folding and Assembly. *Angew. Chem. Int. Ed.*, **2016**, *55*, 4519–4522.

21) Hu, Y.; Xu, W.; Li, G.; Xu, L.; Song, A.; Hao, J. Self-Assembled Peptide Nanofibers Encapsulated with Superfine Silver Nanoparticles via Ag+ Coordination. *Langmuir*, **2015**, *31*, 8599–8605.

22) Jadhav, S. J.; Bandyopadhyay, A.; Gopi, H. N. Protein secondary structure mimetics: Crystal conformations of α/γ4-hybrid peptide 12-helices with proteinogenic side chains and their analogy with α-and β-peptide helices. *Org. Biomol. Chem.*, **2013**, *11*, 509-514.

23) Jadhav, S. V., Misra, R., Singh, S. K., Gopi, H. N. Efficient access to enantiopure γ4-residues with proteinogenic side chains and structural investigation of γ4-Asn and γ4-Ser in hybrid peptide helices. *Chem. Eur. J.*, **2013**, *19*, 16256–16262.